Chemistry contribution to stratospheric ozone depletion after the unprecedented water rich Hunga Tonga eruption

Jun Zhang[1], Douglas Edward Kinnison[2], Yunqian Zhu[3], Xinyue Wang[1], Simone Tilmes[4], Kimberlee Robyn Dubé[5], and William J. Randel[4]

[1]National Center for Atmospheric Research
[2]NCAR/CLAS
[3]University of Colorado Boulder
[4]National Center for Atmospheric Research (UCAR)
[5]University of Saskatchewan

August 8, 2023

Abstract

Following the Hunga Tonga–Hunga Ha'apai (HTHH) eruption in January 2022, stratospheric ozone depletion was observed in the Southern Hemisphere mid-latitudes and Antarctica during the 2022 austral wintertime and springtime. This eruption injected sulfur dioxide and unprecedented amounts of water vapor into the stratosphere. This work examines and quantifies the chemistry contribution of the volcanic materials to the ozone depletion using chemistry-climate model simulations with nudged meteorology. Simulated 2022 ozone and nitrogen oxides (NOx) anomalies show a good agreement with satellite observations. We find that chemistry only contributes up to 6% and 20% ozone destruction at mid-latitudes wintertime and Antarctic springtime respectively. The majority of the ozone depletion is attributed to the internal variability and dynamical changes forced by the eruption. Both the simulation and observations show a significant NOx reduction associated with the HTHH aerosol plume, indicating the enhanced dinitrogen pentoxide hydrolysis on sulfate aerosol.

Chemistry contribution to stratospheric ozone depletion after the unprecedented water rich Hunga Tonga eruption

Authors: Jun Zhang[1*], Douglas Kinnison[1], Yunqian Zhu[2,3], Xinyue Wang[1], Simone Tilmes[1], Kimberlee Dube[4], William Randel[1]

Affiliations:

[1]Atmospheric Chemistry Observations & Modeling Laboratory, National Center for Atmospheric Research, Boulder, CO, USA

[2] Cooperative Institute for Research in Environmental Sciences, University of Colorado Boulder, Boulder, CO, USA, 80309

[3]Chemical Sciences Laboratory, National Oceanic and Atmospheric Administration, Boulder, CO, USA, 80305

[4]Institute of Space and Atmospheric Studies, University of Saskatchewan, Saskatoon, SK, Canada

[*]Corresponding author: Jun Zhang (jzhan166@ucar.edu)

Key Points:

- Nudged chemistry-climate model simulations are used to quantify the chemistry impact on the stratospheric ozone following the Hunga Tonga-Hunga Ha'apai eruption.
- The modeled ozone and nitrogen oxides anomalies show a good agreement with satellite observations.
- Chemistry contributes to 6% and 20% ozone depletion at mid-latitudes and Antarctica, respectively.

Abstract

Following the Hunga Tonga–Hunga Ha'apai (HTHH) eruption in January 2022, stratospheric ozone depletion was observed in the Southern Hemisphere mid-latitudes and Antarctica during the 2022 austral wintertime and springtime. This eruption injected sulfur dioxide and unprecedented amounts of water vapor into the stratosphere. This work examines and quantifies the chemistry contribution of the volcanic materials to the ozone depletion using chemistry-climate model simulations with nudged meteorology. Simulated 2022 ozone and nitrogen oxides (NO_x) anomalies show a good agreement with satellite observations. We find that chemistry only contributes up to 6% and 20% ozone destruction at mid-latitudes wintertime and Antarctic springtime respectively. The majority of the ozone depletion is attributed to the internal variability and dynamical changes forced by the eruption. Both the simulation and observations show a significant NOx reduction associated with the HTHH aerosol plume, indicating the enhanced dinitrogen pentoxide hydrolysis on sulfate aerosol.

Plain language summary

The January 2022 eruption of the Hunga Tonga-Hunga Ha'apai underwater volcano injected a large amount of water vapor (H_2O) and moderate amounts of sulfur dioxide (SO_2) into the stratosphere. Stratospheric ozone losses were observed following the eruption in the Southern Hemisphere (SH) mid-latitudes and Antarctica during the 2022 austral wintertime and springtime. The ozone layer in the stratosphere protects Earth's human being and biosphere from harmful ultraviolet light by absorbing the harmful portion of the radiation from the sun. We use computer simulation in this study to examine the impacts of chemical processes on the ozone layer from the volcanic materials. We find that chemistry is contributing up to 6% and 20% of the ozone reduction at SH mid-latitudes winter and Antarctic spring respectively. The majority of ozone changes are due to transport and dynamical processes from internal variability in the climate system and forced response by the HTHH eruption.

1. Introduction

It has been long known that explosive volcanic eruptions can cause stratospheric ozone depletion by injecting sulfate and its precursor SO_2 into the stratosphere, which enhances aerosol surface areas for heterogeneous chemistry (Hofmann & Solomon, 1989; Portmann et al., 1996; Kinnison et al., 1994; Solomon et al., 1996, 1998). Observations have shown that Antarctic ozone depletion was enhanced after the major eruption of Mount Pinatubo in the early 1990s with injections of ~18 Tg sulfur dioxide (SO_2) (e.g., Read et al., 1993; Krueger et al., 1995; Solomon et al., 2005). Even the moderate magnitude volcanic eruption of Calbuco in 2015, which injected 0.4 Tg of SO_2, exacerbated ozone depletion, producing a record-breaking October ozone hole that lasted late into the season (Solomon et al., 2016; Ivy et al., 2017; Stone et al., 2017; Zhu et al., 2018).

The January 2022 Hunga Tonga–Hunga Ha'apai (HTHH) eruption was an unprecedented underwater volcanic event of the modern era, which injected volcanic materials to altitudes up to 58 km in the mesosphere (Carr et al., 2022; Proud et al., 2022). Unlike land-based volcanoes such as Mount Pinatubo and Calbuco, HTHH injected about 150 Tg of water (H_2O) (Xu et al., 2022; Millán et al., 2022) along with 0.4 to 0.5 Tg SO_2 into the stratosphere (Carn et al. 2022; Taha et al., 2022). This H_2O injection increased the global stratospheric water burden by more than 10% (Vömel et al., 2022; Khaykin et al., 2022; Randel et al., 2023). The additional source of H_2O can impact the ozone chemistry by altering the HOx chemical cycles, heterogeneous reaction rate, and the Polar Stratospheric Cloud formation (PSCs) (Solomon et al., 1997; Anderson et al., 2012). In addition, volcanic aerosols provide extra surface area density (SAD) for heterogeneous reactions affecting ozone chemistry, and suppressing the NOx-Ox cycles (defined later in Section 3.2) (Tie and Brasseur, 1995).

Previous studies have utilized the chemistry-climate model Community Earth System Model Version 2 (CESM2) with Whole Atmosphere Community Climate Model Version 6 (WACCM6) to simulate the dispersion and evolution of aerosol and water plumes after the HTHH eruption (Zhu et al., 2022; Wang et al., 2023, Lu et al., 2023). WACCM6 simulations reproduced the Microwave Limb Sounder (MLS) observed evolution of the H_2O throughout 2022 and the stratospheric cooling and circulation changes as seen by European Center for Medium Range Forecasts ERA5 reanalysis (Wang et al., 2023). Zhu et al. (2022) found that the additional water

vapor increases hydroxide, halves the sulfur dioxide lifetime, promotes faster sulfate aerosol formation as seen by Cloud-Aerosol Lidar and Infrared Pathfinder Satellite Observation (CALIPSO) and The Ozone Mapping and Profiler Suite Limb Profiler (OMPS-LP), and leads to the increased aerosol optical depth and radiation effect. The persistent perturbations in H_2O and aerosol due to HTHH plumes in the SH stratosphere throughout 2022 draw attention to exploring the SH stratospheric ozone response.

Lu et al. (2023) explored the ozone response to the HTHH eruption considering 0.4 Tg SO_2 emission but ignored the large H_2O injection. Wang et al. (2023) simulated large stratospheric ozone anomalies in mid-latitudes and Antarctica in 2022 as observed by MLS. Manney et al. (2023) looked into the nitrous oxide anomalies with ozone and suggested that transport plays a role in the ozone reduction. However, the relative effects of chemistry and dynamics on these ozone anomalies has not been quantified. This work aims to examine and quantify the chemical ozone depletion and the associated chemical processes in the wake of HTHH. We isolate the ozone impact owing to chemistry by nudging the model dynamics to meteorology analysis fields.

2. Data and Model

2.1 Microwave Limb Sounder (MLS)

The MLS instrument was launched on NASA's EOS Aura satellite on July 15, 2004. For the past 19 years, MLS has provided a uniquely comprehensive suite of daily global measurements for studying lower stratospheric chemical processing. MLS Version 5.0 data is used in this work. The standard product for O_3 is derived from MLS radiance measurements near 240 GHz; the O_3 data and its validation are described by Livesey et al. (2020). The useful data range is from 261 hPa up to 0.001 hPa. Here the O_3 data used are compiled into a daily zonal means at a resolution of 2.5° latitude from 2004 to 2022. Anomalies for 2022 shown in this study are calculated based on climatology background from 2007 to 2021, as the model simulations started from 2007.

2.2 Optical Spectrograph and InfraRed Imager System (OSIRIS)

The Optical Spectrograph and InfraRed Imager System (OSIRIS) has been in sun-synchronous orbit on the Odin satellite since 2001 (Llewellyn et al., 2004; Murtagh et al., 2002). The optical spectrograph scans the atmospheric limb to measure vertical profiles of limb-scattered solar irradiance between 275 and 810 nm. There are between 100 and 400 profiles per day, depending on the time of year and the scanning range. Only the descending node measurements are considered here due to a drift in the orbit that has caused inconsistent ascending node sampling over the course of the mission. We use NOx from version 7.2 of the OSIRIS retrieval, which is described and validated in Dubé et al. (2022). The OSIRIS NO_2 observations are converted to NOx using the PRATMO photochemical box model (Prather and Jaffe, 1990; McLinden et al., 2000), following the process in Dubé et al. (2020). PRATMO is also used to scale the OSIRIS measurements to a common local solar time of 12:00 pm in order to account for variations in the measurement time caused by the processing satellite orbit, which is described in Dubé et al. (2020).

2.3 Whole Atmosphere Community Climate Model (WACCM)

The CESM2/WACCM6 was used to conduct the numerical experiments. This state-of-the-art chemistry-climate model extends from the Earth's surface to approximately 140 km and includes comprehensive troposphere-stratosphere-mesosphere-lower-thermosphere (TSMLT) chemistry (details described in Gettelman et al., 2019). WACCM6 includes a prognostic stratospheric aerosol

module (Mills et al., 2016) and has been utilized extensively to study volcanic aerosols and their impact on climate change and ozone losses (e.g., Mills et al., 2017; Stone et al., 2017; Zambri et al., 2019). In this study, the simulations feature a horizontal resolution of 0.9° latitude × 1.25° longitude using the finite volume dynamical core (Lin & Rood, 1996), and 110 vertical levels, with a vertical resolution of ~500m in the upper troposphere and lower stratosphere. WACCM6 is run in a specified dynamics configuration (WACCM6-SD), where the temperatures and winds are relaxed to Modern-Era Retrospective analysis for Research and Applications Version 2 (MERRA-2) reanalyses (Gelaro et al., 2017) using a relaxation time of 50 hours. This configuration starts from 2007 until the end of 2022, using initial conditions from a long historical simulation (Gettelman et al., 2019). Starting in January 2022, we conduct two cases: the experiment case with full forcing (SO_2 and H_2O injection) from the HTHH eruption (as defined in Zhu et al., 2022) and the control case with no forcing (no SO_2 or H_2O injection) from HTHH eruption. The difference between these two nudged simulations gives information about the chemistry contribution to the stratospheric ozone depletion after the HTHH eruption. We use the emission described in Zhu et al. (2022), where 150 Tg of H_2O and 0.42 Tg of SO_2 are injected on January 15, 2022, from ~20 to 35 km.

3. Results and Discussions

3.1 Observed and simulated ozone anomaly from MLS and WACCM6-SD

It is expected that the large HTHH H_2O and aerosol perturbations can impact stratospheric dynamics and chemistry, and hence ozone abundances. Figure 1 shows MLS observed ozone from 2004 to 2022 and WACCM6-SD simulated ozone during 2022 in the stratosphere. MLS satellite observations indicate anomalous negative ozone in 2022 both over SH midlatitudes and tropics (10°S-60°S) in winter as well as Antarctica (60°S-82°S) in spring. The MLS ozone concentration over 10°S-60°S shows a record low relative to the climatology period (2004 to 2022) in the SH austral winter (Fig. 1a, red line) at 30 hPa. Large midwinter interannual variability in this region is linked to the Quasi-Biennial Oscillation (QBO), as discussed in Wang et al. (2023). MLS also shows a relatively deep ozone hole in the SH austral spring (Fig. 1b) at 80 hPa. The negative ozone anomaly over the polar region (60°S-82°S) is large in October-December, but within the variability of previous years. This is because the climatology period (2004 to 2022) also includes years with either relatively strong polar vortex or volcanic impact. For example, the lowest line in Figure 1b is in the year 2015, when a record October ozone hole occurred after the Calbuco volcanic eruption (Solomon et al., 2015; Ivy et al., 2017). The accuracy of MLS O_3 is about 0.2 ppmv at 30 hPa and 0.1 ppmv near 80 hPa (Livesey et al., 2020). The difference between MLS climatology mean and 2022 is outside the MLS ozone systematic error during June-August in Fig. 1a and October in Fig. 1b, which reinforces the anomalous low ozone occurring in the SH mid-latitudes winter and Antarctica spring 2022. WACCM6-SD captures both the record low ozone over 10°S-60°S and the large ozone anomaly over 60°S-82°S, and is within the systematic error of MLS, except in December 2022 in Fig. 1b.

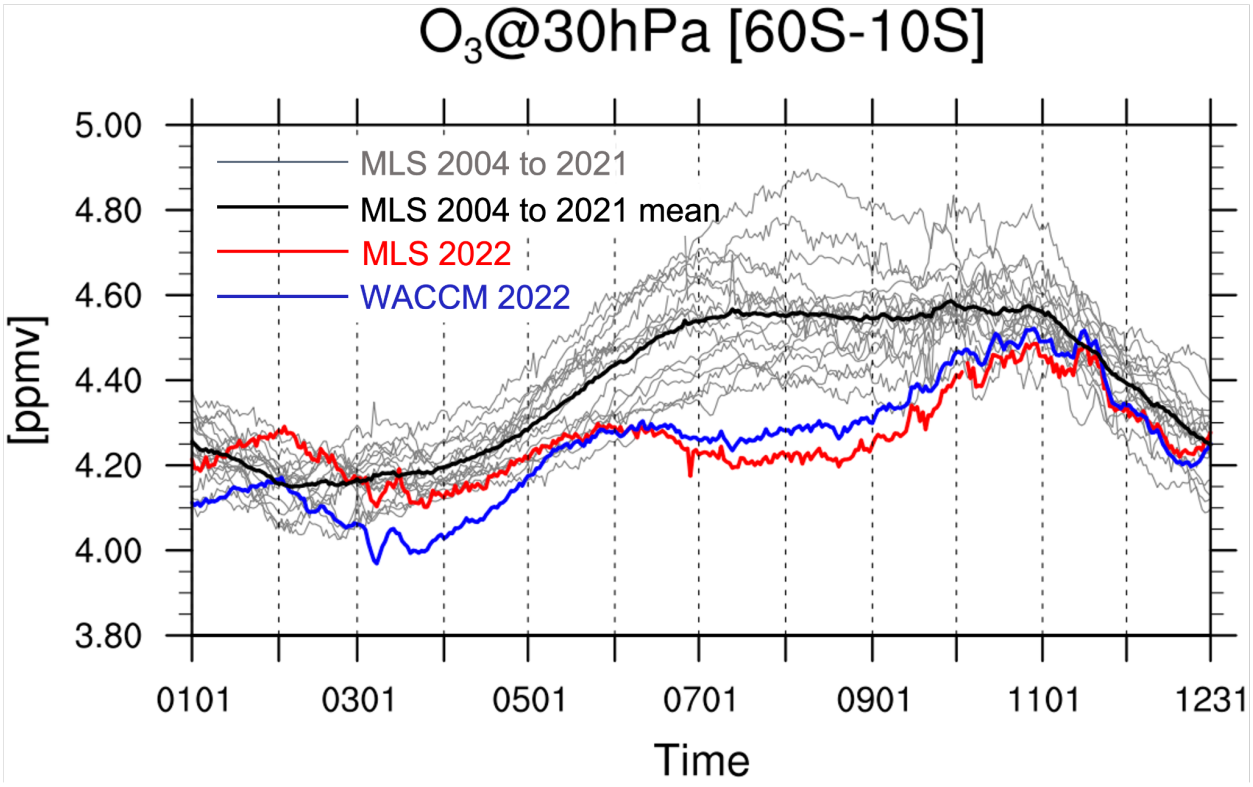
O3@30hPa [60S-10S]
MLS 2004 to 2021
MLS 2004 to 2021 mean
MLS 2022
WACCM 2022
[ppmv]
5.00
4.80
4.60
4.40
4.20
4.00
3.80
0101
0301
0501
0701
0901
1101
1231
Time

(a)

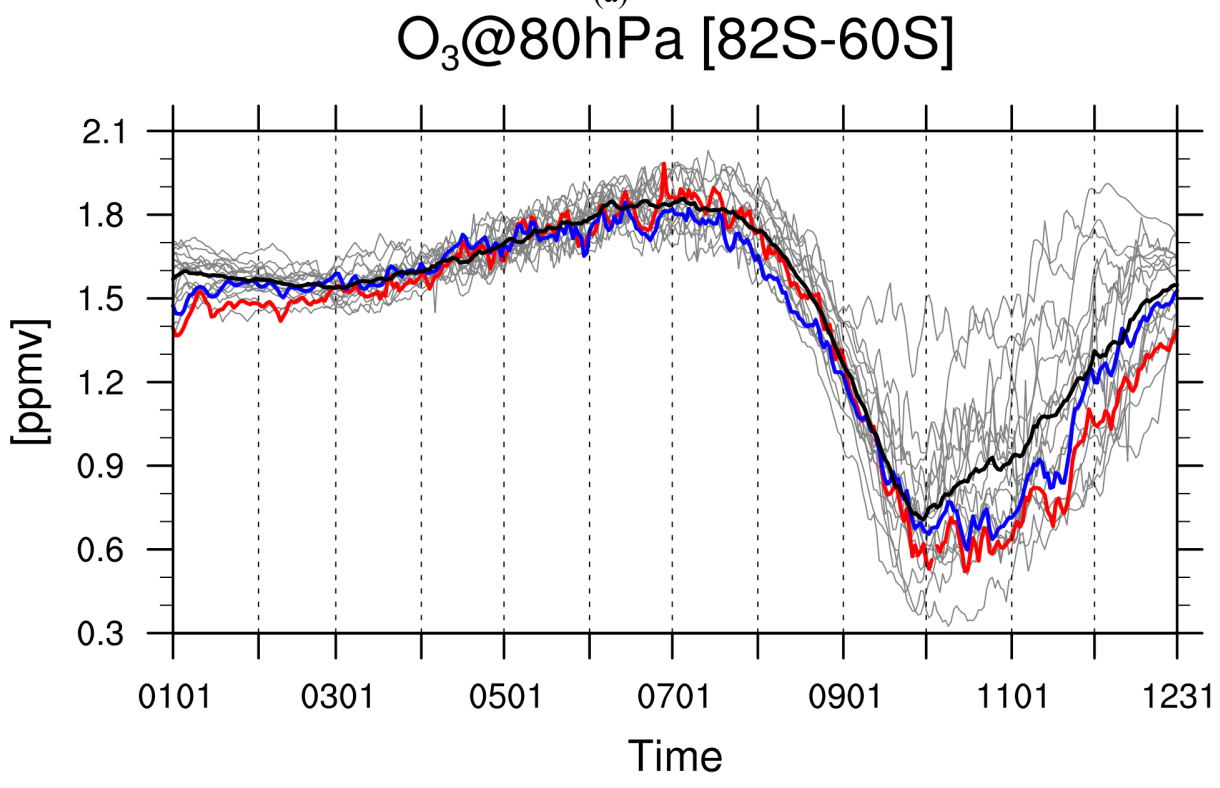
O3@80hPa [82S-60S]
[ppmv]
2.1
1.8
1.5
1.2
0.9
0.6
0.3
0101
0301
0501
0701
0901
1101
1231
Time

(b)

Figure 1. Time series of ozone concentration (ppmv) for (a) midlatitudes and tropics (10°S-60°S) at 30 hPa and (b) polar region (60°S-82°S) at 80 hPa from MLS and WACCM. MLS observations are shown from 2004 to 2022. Gray lines show time serieses of MLS ozone during 2004-2021 and the black line indicates the mean MLS ozone over the climatology. The red and blue lines are for MLS and WACCM6-SD ozone in 2022, respectively.

3.2 Quantifying the chemical contribution to the ozone reduction

Stratospheric ozone changes in 2022 compared with the climatology can be attributed to various factors: internal variability in the climate system (e.g., QBO), and forced changes after the HTHH eruption including both dynamics and chemistry impacts. Both observed and simulated 2022 anomalies showing in the following are calculated as deviations from the 2007-2021 background instead of 2004-2021 to be consistent with model simulation period. We note that the difference of the derived 2022 anomaly between using 2004 and 2007 is minimal. The derived ozone anomaly from MLS and WACCM6-SD in August are shown in Figure 2a and 2b. The lower stratospheric wintertime SH mid-latitude ozone reduction is well represented in WACCM6-SD, along with the ozone increase in the tropics, which is related to the QBO. These ozone anomalies are the result of the combination of internal variability and HTHH eruption forced changes. Figure 2c shows the ozone changes due to chemistry only, calculated by taking the difference between the full forcing experiment run (SO_2+H_2O) and the no forcing control run in 2022. The blue and red contour lines highlight the location of HTHH water and aerosol plumes, which reveals the separation of the H_2O and aerosol plumes over time due to the sedimentation of the aerosols (Legras et al. 2022, Wang et al., 2023). As the experiment and control simulations are nudged to the same dynamics, the ozone changes in Figure 2c are purely due to the chemistry impact from the enhanced water and aerosol SAD perturbation. The ozone depletion over the SH mid-latitudes ranges from 200 hPa up to 30 hPa. In particular, the reduction at 30 to 50 hPa and 100 to 200 hPa are outside of previous variability (hatched region), with the peak reaching about 20% ozone reduction. Chemistry only contributes up to 6% of ozone depletion at mid-latitudes near 70 hPa (Fig. 2c). Consequently, less than 30% of the ozone reduction at the hatched regions in Figure 2a and 2b is attributed to chemistry, with the other changes a result of dynamical changes due to internal variability from QBO and forced dynamical response to the HTHH eruption.

In the springtime (October-December) of the Antarctic polar region, a large negative ozone anomaly is observed within the polar vortex (south of 60˚S) in 2022 (Fig. 2d), even though it is not a record-breaking low ozone hole (not hatched). WACCM6-SD reproduces this large ozone reduction in general, but slightly underestimates the ozone loss between 30 to 50 hPa (Fig. 2e). The simulation (Fig. 2f) shows that the aerosol plume from the HTHH eruption entered the Antarctic near the bottom of the polar vortex (~100 hPa) in October. However, the water plume was confined outside of the polar vortex due to the strong polar jet stream near 25 km (Schoeberl et al. 2023; Manney et al, 2023; Wang et al., 2023). Note that although the simulated HTHH aerosol penetrated across the bottom of the polar vortex, it is difficult to prove it with observations. Enhanced polar extinction in OMPS-LP measurements can be due to polar stratospheric clouds in the winter season (Manney et al., 2023; Wang et al., 2023). In addition, the amount of sulfate entering the polar vortex in the simulation is relatively small (only double the background), and satellite observations (e.g., CALIPSO lidar) sometimes cannot capture it due to background noise

level. The ozone depletion simulated in Figure 2f is because the volcanic aerosol entered the bottom of the polar vortex which provides additional SAD for heterogeneous chemistry in the polar region. Chemistry (Fig. 2f) leads to ~ 20% ozone reduction (this is equivalent to about 40% of the total ozone depletion) near the center of the Antarctic vortex.

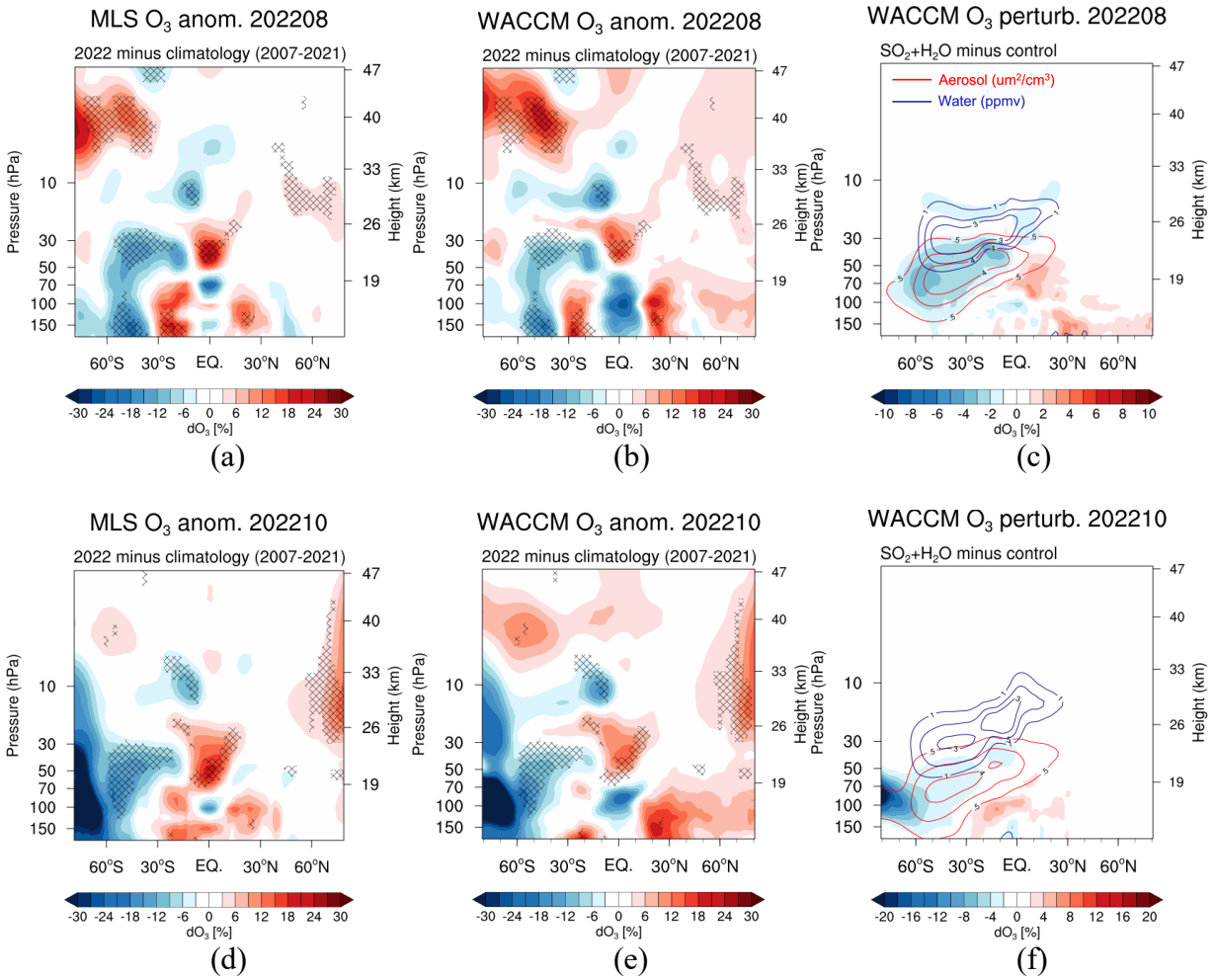

Figure 2. Percentage change of 2022 ozone anomaly (%) relative to climatology (2007 to 2021) from MLS (a) and WACCM6-SD (b) in August. (d) and (e) are the same but for October. Hatched regions indicate where the 2022 anomalies are outside the range of all variability during 2007-2021. Percentage change of ozone (%) calculated from full-forcing (SO_2+H_2O) compared to no-forcing control runs in August (c) and October (f). The blue and red contour lines in (c) and (f) are water anomaly in ppmv and aerosol surface area density anomaly in um^2/cm^3, respectively. Note that panel c and f have different color bar ranges from panel a, b, d, e.

We characterize the major chemical processes that lead to the 6% and 20% of chemical ozone depletion in the mid-latitudes and polar regions discussed above. The chemical destruction of odd oxygen (Ox = O_3 + O + $O(^1D)$ + other terms; Brasseur & Solomon, 2005) is directly linked to ozone abundance in the stratosphere. Different Ox catalytic destruction cycles involve nitrogen oxides (NOx-Ox), hydrogen radicals (HOx-Ox), halogen oxides (ClOx/BrOx-Ox) as well as the chemical loss by the Chapman self-destruction mechanism (Ox-Ox) (e.g., Crutzen & Ehhalt, 1977;

Solomon, 1999). Supplementary Text S1 defines the odd oxygen used in this study and the reactions that are contained in each odd oxygen chemical family. Figure 3a and 3b characterize the total Ox loss (sum of Ox-Ox, NOx-Ox, HOx-Ox and ClOx/BrOx-Ox cycles) during the SH winter and spring. The changes in Ox are induced by the addition of water and aerosol injection from HTHH eruption. In the wintertime, the major Ox loss occurs in the mid-latitudes from 150 to 20 hPa, consistent with the location of major ozone loss in Figure 2c. During springtime, the total Ox loss extends into the polar region, associated with the aerosol plume shown in Figure 2f.

The vertical profile of changes in individual loss cycles are illustrated in Figure 3c and 3d for mid-latitudes winter and Antarctic spring, respectively. Increasing aerosol surface areas decrease the abundance of NOx and hence the NOx-catalyzed ozone destruction cycles (red lines) (discussed in section 3.3). Both HOx-Ox and ClOx/BrOx-Ox cycles play important roles in the chemical ozone destruction for mid-latitudes winter, but at different altitudes. The HOx-Ox cycle is more significant at 20 to 30 km, while the ClOx/BrOx-Ox cycle plays a larger role below 20 km. The enhanced HOx cycle is the combined results of direct water injection and the HOx repartitioning induced from NOx reduction (Wennberg et al., 1994; Solomon et al., 1996). The reduced NOx also gives rise to ClOx enhancement as ClOx is inversely correlated with NOx (Stimpfle et al., 1994; Solomon et al., 1999). In the Antarctic spring, ClOx/BrOx-Ox cycle controls the behavior of total Ox change below around 18 km. HOx-Ox loss cycle is still the major loss mechanism at 20 to 25 km. However, this loss is largely offset by hindered NOx-Ox loss, which is normally the most important loss cycle at this altitude in the background atmosphere (Zhang et al., 2021). It is eye-catching to see there is a negative Ox perturbation at around 16-18 km, corresponding to 70-100 hPa in Figure 2b. This is because the ozone abundances in the experiment run drop to extreme low values at 70-100 hPa in the core of the vortex, hence the formation of ClO (and therefore chlorine nitrate $ClONO_2$) is impeded (Fig. S1). Rapid deactivation of Cl into hydrochloric acid (HCl) then occurs even if the enhanced SAD are still present and temperatures are very cold (Douglass et al., 1995; Solomon et al., 2015). This rapid deactivation suppresses the Ox loss due to ClOx/BrOx-Ox cycle in the experiment run compared to the control run. Figure 3c and 3d indicate that the reaction rates of all the Ox chemical loss cycles are modified even though only SO_2 and H_2O emissions are injected into the atmosphere from the HTHH eruption. This is expected since these cycles couple to each other and change repartitioning from each other.

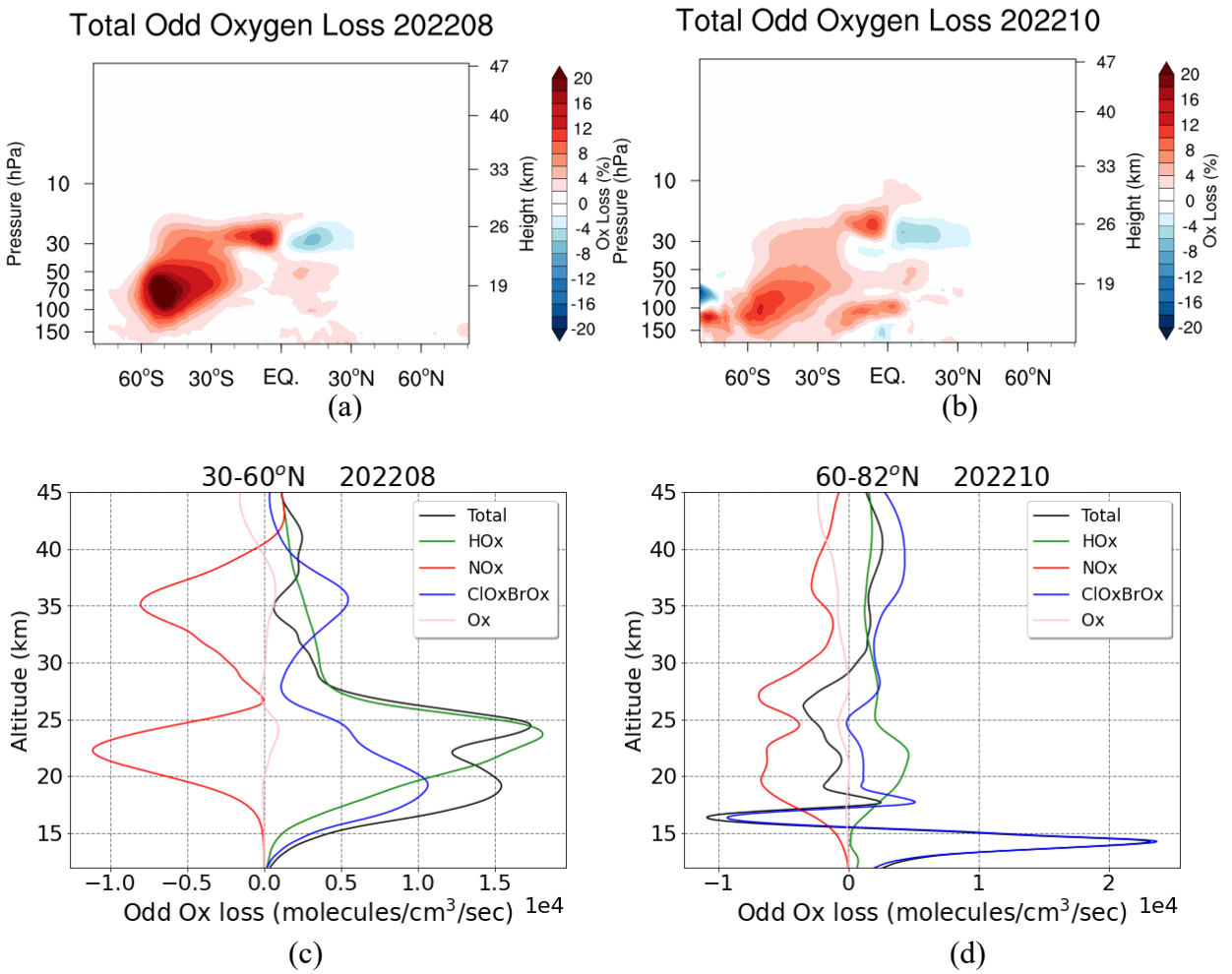

Figure 3. Calculated perturbations from full-forcing (SO_2+H_2O) experiment run compared to no-forcing control run for total OddOx loss in August (a) and October (b). Vertical profile of total Odd oxygen (Ox) loss (in black) and the loss from individual cycles of HOx-Ox, NOx-Ox, ClOxBrOx-Ox and Ox-Ox at mid-latitudes in August (c) and Antarctic region in October (d).

3.3 Negative NOx anomaly after HTHH eruption

NOx reduction is expected following large volcanic eruptions, which perturbs ozone abundance in the stratosphere (e.g., Fahey et al., 1993; Mills et al., 1993; Berthet et al., 2017; Zambri et al., 2019). Figure 4 examines the NOx anomaly after the HTHH eruption from OSIRIS observations and WACCM6-SD model simulations. A dipole pattern is observed both in the OSIRIS and WACCM: a NOx reduction at around 25 km and below, and a positive anomaly above. This positive anomaly is mainly due to the QBO internal variability, as it is also seen in 2008 when the QBO phase is similar to 2022 while the negative anomaly is not found (Fig. S2) (Park et al., 2017). Figure 4a and 4d show the OSIRIS observed NOx anomalies in August and October 2022, with reductions of 30~40% over the mid-latitude lower stratosphere. This negative anomaly is approximately collocated with the HTHH aerosol plume in Figure 2c and 2f, which is consistent with the plume location shown in Wang et al. (2023) from the OMPS-LP data. The HTHH aerosol

reduce the NOx abundance via the well-known heterogeneous chemical reactions dinitrogen pentoxide (N_2O_5) hydrolysis on aerosols (e.g., Hofmann and Solomon, 1989; Solomon, 1999; Berthet et al., 2017). Due to the N_2O_5 hydrolysis on the surface of aerosol, nitric acid (HNO_3) formation is promoted which acts as a major sink of NOx in the atmosphere during night-time. We note that OSIRIS data show strong NOx decreases throughout 2022 (not shown) that overlap the HTHH aerosol layer, but OSIRIS does not have high latitude measurements during midwinter. Model calculations (Fig. 4b and 4e) show NOx decreases in the lower stratosphere that are similar in magnitude (~30-40%) and location to the OSIRIS results, demonstrating that the NOx-aerosol reactions are captured well in the model. Figure 4c and 4f denote the modeled changes in N_2O_5 hydrolysis rate overlying with aerosol SAD anomaly due to the HTHH eruption, derived from the difference between full-forcing (SO_2+H_2O) and no-forcing control runs. This heterogeneous chemical reaction rate is enhanced by more than 50% at the location where the maximum of NOx reduction occurs in Figure 4b and 4e. The results shown here are consistent with the conclusion drawn from Santee et al. (2023) using MLS data, suggesting the hydrolysis of N_2O_5 is the primary mechanism for the reduction of NOx. We note that even though this NOx reduction is significant, we found that the NOx impact on ozone is largely canceled by HOx-Ox and ClOx-Ox cycles as shown in Figure 3c and 3d.

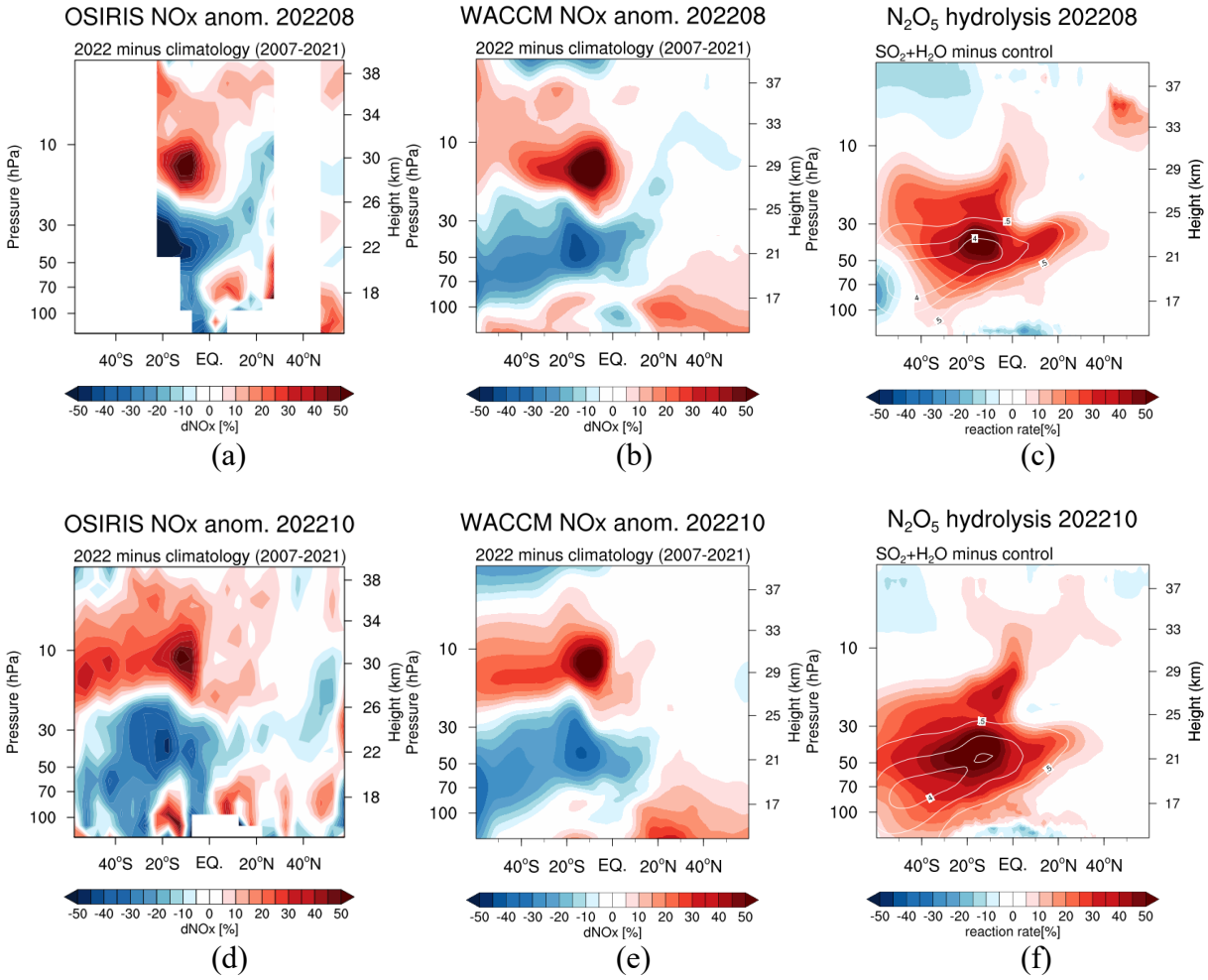

Figure 4. Calculated NOx anomaly (%) relative to climatology (2007 to 2021) from OSIRIS and WACCM6-SD in August and October (a), (b) and (d), (e). Calculated changes (%) in N_2O_5 hydrolysis rate on sulfate aerosols in the WACCM6-SD model from full-forcing (SO_2+H_2O) compared to no-forcing control runs in August and October (c) and (f). The white contour line in (c) and (f) is the aerosol surface area density anomaly in um^2/cm^3.

4. Summary and discussion

The January 2022 Hunga Tonga-Hunga Ha'apai eruption injected ~150 Tg of water and ~0.42 Tg SO_2 into the SH stratosphere. MLS observed ozone reductions in the SH stratosphere mid-latitudes and Antarctica during the 2022 austral wintertime and springtime. This work focuses on examining and quantifying the chemical ozone depletion due to the SO_2 and H_2O injection. We use WACCM6-SD nudged simulations to disentangle the role of chemistry from that of dynamics. WACCM6-SD shows a good agreement with MLS ozone anomaly and also reproduces the NOx anomaly in 2022 compared to OSIRIS measurements.

We found chemistry contributes to 6% and 20% ozone depletion at mid-latitudes and Antarctica, respectively. The majority of ozone changes are due to transport and dynamical processes from internal variability in the climate system and forced response by the HTHH eruption. One caveat is that the chemistry quantified here does not include the dynamics feedback on the chemistry. For example, water can cool the stratosphere, which would further promote heterogeneous reactions. However, because these two simulations conducted here are nudged to the same dynamics, the temperature is not allowed to change to reflect the feedback on chemistry. To characterize the chemical processes that contributed to the ozone loss, different loss cycles (NOx-Ox, HOx-Ox, ClOx/BrOx-Ox and Ox-Ox) were examined and their relative significance to the ozone depletion at SH mid-latitudes and Antarctica were evaluated. We found both HOx-Ox and ClOx/BrOx-Ox cycles play important roles in the total chemical ozone destruction for mid-latitudes winter. While during the Antarctic spring, ClOx/BrOx-Ox cycle is dominant and controls the behavior of total Ox change in the lower stratosphere. We also document that both OSIRIS and WACCM6-SD show a NOx reduction that collocates with HTHH aerosols plume, demonstrating the enhanced N_2O_5 hydrolysis on sulfate aerosol. Consequently, the NOx-Ox loss cycle is strongly suppressed associated with the significant NOx reduction. However, the NOx impact on ozone is minimal since it is largely canceled by HOx-Ox and ClOx/BrOx-Ox cycles.

Acknowledgments

Jun Zhang and Xinyue Wang are supported by the NSF via NCAR's Advanced Study Program Postdoctoral Fellowship. Douglas Kinnison is partially supported by NASA grant no. 80NSSC19K0952. NCAR's Community Earth System Model project is supported primarily by the National Science Foundation. This material is based upon work supported by the National Center for Atmospheric Research, which is a major facility sponsored by the NSF under Cooperative Agreement No. 1852977. Computing and data storage resources, including the Cheyenne supercomputer (doi:10.5065/D6RX99HX), were provided by the Computational and Information Systems Laboratory (CISL) at NCAR. The authors thank the Swedish National Space Agency and the Canadian Space Agency for the continued operation and support of Odin-OSIRIS. Kimberlee

Dube is supported by the Canadian Space Agency (grant no. 21SUASULSO). This project received funding from NOAA's Earth Radiation Budget (ERB) Initiative (CPO #03-01-07-001). Yunqian Zhu is supported in part by NOAA cooperative agreements NA17OAR4320101 and NA22OAR4320151.

Open Research

CESM2/WACCM6 is an open-source community model, which was developed with support primarily from the National Science Foundation. WACCM6 source code can be downloaded at https://www.cesm.ucar.edu/models/cesm2/download. Figures in this study are plotted by using NCAR Command Language (NCL) and Python. The related code can be found in NCL application examples (https://www.ncl.ucar.edu/Applications/). Python is an open-source programming language.

References

Anderson, J. G., Wilmouth, D. M., Smith, J. B., & Sayres, D. S. (2012). UV dosage levels in summer: Increased risk of ozone loss from convectively injected water vapor. *Science*, 337(6096), 835-839. DOI: 10.1126/science.1222978. DOI: 10.1126/science.1222978

Berthet, G., Jégou, F., Catoire, V., Krysztofiak, G., Renard, J. B., Bourassa, A. E., ... & Guimbaud, C. (2017). Impact of a moderate volcanic eruption on chemistry in the lower stratosphere: balloon-borne observations and model calculations. *Atmospheric Chemistry and Physics*, 17(3), 2229-2253. https://doi.org/10.5194/acp-17-2229-2017

Brasseur, G. P., & Solomon, S. (2005). Aeronomy of the middle atmosphere: Chemistry and physics of the stratosphere and mesosphere (Vol. 32). *Springer Science & Business Media*.

Carn, S. A., Krotkov, N. A., Fisher, B. L., & Li, C. (2022). Out of the blue: Volcanic SO2 emissions during the 2021–2022 eruptions of Hunga Tonga—Hunga Ha'apai (Tonga). *Frontiers in Earth Science*, 10, 976962. https://doi.org/10.3389/feart.2022.976962

Carr, J. L., Horváth, Á., Wu, D. L., & Friberg, M. D. (2022). Stereo plume height and motion retrievals for the record-setting Hunga Tonga-Hunga Ha'apai eruption of 15 January 2022. *Geophysical Research Letters*, 49(9), e2022GL098131. https://doi.org/10.1029/2022GL098131

Crutzen, P. J., & Ehhalt, D. H. (1977). Effects of nitrogen fertilizers and combustion on the stratospheric ozone layer. *Ambio*, 112-117.

Douglass, A. R., Schoeberl, M. R., Stolarski, R. S., Waters, J. W., Russell III, J. M., Roche, A. E., & Massie, S. T. (1995). Interhemispheric differences in springtime production of HCl and ClONO2 in the polar vortices. *Journal of Geophysical Research: Atmospheres*, 100(D7), 13967-13978. https://doi.org/10.1029/95JD00698

Dubé, K., Randel, W., Bourassa, A., Zawada, D., McLinden, C., & Degenstein, D. (2020). Trends and variability in stratospheric NOx derived from merged SAGE II and OSIRIS satellite observations. *Journal of Geophysical Research: Atmospheres*, 125(7), e2019JD031798. https:// doi.org/10.1029/2019JD031798

Dubé, K., Zawada, D., Bourassa, A., Degenstein, D., Randel, W., Flittner, D., Sheese, P., and Walker, K.: An improved OSIRIS NO2 profile retrieval in the upper troposphere–lower stratosphere and intercomparison with ACE-FTS and SAGE III/ISS, *Atmos. Meas. Tech*., 15, 6163–6180, https://doi.org/10.5194/amt-15-6163-2022, 2022.

Fahey, D. W., Kawa, S. R., Woodbridge, E. L., Tin, P., Wilson, J. C., Jonsson, H. H., ... & Chan, K. R. (1993). In situ measurements constraining the role of sulphate aerosols in mid-latitude ozone depletion. *Nature*, 363(6429), 509-514. https://doi.org/10.1038/363509a0

Gelaro, R., McCarty, W., Suárez, M. J., Todling, R., Molod, A., Takacs, L., ... & Zhao, B. (2017). The modern-era retrospective analysis for research and applications, version 2 (MERRA-2). *Journal of climate*, 30(14), 5419-5454. https://doi.org/10.1175/JCLI-D-16-0758.1

Gettelman, A., Mills, M. J., Kinnison, D. E., Garcia, R. R., Smith, A. K., Marsh, D. R., ... & Randel, W. J. (2019). The whole atmosphere community climate model version 6 (WACCM6). *Journal of Geophysical Research: Atmospheres*, 124(23), 12380-12403. https://doi.org/10.1029/2019JD030943

Hofmann, D. J., & Solomon, S. (1989). Ozone destruction through heterogeneous chemistry following the eruption of El Chichon. *Journal of Geophysical Research: Atmospheres*, 94(D4), 5029-5041. https://doi.org/10.1029/JD094iD04p05029

Khaykin, S., Podglajen, A., Ploeger, F., Grooß, J. U., Tencé, F., Bekki, S., ... & Ravetta, F. (2022). Global perturbation of stratospheric water and aerosol burden by Hunga eruption. *Communications Earth & Environment*, 3(1), 316. https://doi.org/10.1038/s43247-022-00652-x

Kinnison, D. E., Grant, K. E., Connell, P. S., Rotman, D. A., & Wuebbles, D. J. (1994). The chemical and radiative effects of the Mount Pinatubo eruption. *Journal of Geophysical Research: Atmospheres*, 99(D12), 25705-25731. https://doi.org/10.1029/94JD02318

Krueger, A. J., Walter, L. S., Bhartia, P. K., Schnetzler, C. C., Krotkov, N. A., Sprod, I. T., & Bluth, G. J. S. (1995). Volcanic sulfur dioxide measurements from the total ozone mapping spectrometer instruments. *Journal of Geophysical Research*: Atmospheres, 100(D7), 14057-14076. https://doi.org/10.1029/98GL00178

Ivy, D. J., Solomon, S., Kinnison, D., Mills, M. J., Schmidt, A., & Neely III, R. R. (2017). The influence of the Calbuco eruption on the 2015 Antarctic ozone hole in a fully coupled chemistry-climate model. *Geophysical Research Letters*, 44(5), 2556-2561. https://doi.org/10.1002/2016GL071925

Legras, B., Duchamp, C., Sellitto, P., Podglajen, A., Carboni, E., Siddans, R., ... & Ploeger, F. (2022). The evolution and dynamics of the Hunga Tonga–Hunga Ha'apai sulfate aerosol plume in the stratosphere. *Atmospheric Chemistry and Physics*, 22(22), 14957-14970. https://doi.org/10.5194/acp-22-14957-2022

Lin, S. J., & Rood, R. B. (1996). Multidimensional flux-form semi-Lagrangian transport schemes. *Monthly Weather Review*, 124(9), 2046-2070. https://doi.org/10.1175/1520-0493(1996)124<2046:MFFSLT>2.0.CO;2

Livesey, N J, W G Read, P A Wagner, L Froidevaux, M L Santee, and M J Schwartz. 2020. "Version 5.0 x Level 2 and 3 Data Quality and Description Document (Tech. Rep. No. JPL D-105336 Rev. A)." *Jet Propulsion Laboratory*.

Llewellyn, E. J., Lloyd, N. D., Degenstein, D. A., Gattinger, R. L., Petelina, S. V., Bourassa, A. E., Wiensz, J. T., Ivanov, E. V., McDade, I. C., Solheim, B. H., McConnell, J. C., Haley, C. S., von Savigny, C., Sioris, C. E., McLinden, C. A., Griffioen, E., Kaminski, J., Evans, W. F., Puckrin, E., Strong, K., Wehrle, V., Hum, R. H., Kendall, D. J., Matsushita, J., Murtagh, D. P., Brohede, S., Stegman, J., Witt, G., Barnes, G., Payne, W. F., Piché, L., Smith, K., Warshaw, G., Deslauniers, D. L., Marchand, P., Richardson, E. H., King, R. A., Wevers, I., McCreath, W., Kyrölä, E., Oikarinen, L., Leppelmeier, G. W., Auvinen, H., Mégie, G., Hauchecorne, A., Lefèvre, F., de La Nöe, J., Ricaud, P., Frisk, U., Sjoberg, F., von Schéele, F., and Nordh, L.: The OSIRIS instrument on the Odin spacecraft, *Can. J. Phys.*, 82, 411–422, https://doi.org/10.1139/p04-005, 2004.

Lu, J., Lou, S., Huang, X., Xue, L., Ding, K., Liu, T., ... & Ding, A. (2023). Stratospheric Aerosol and Ozone Responses to the Hunga Tonga-Hunga Ha'apai Volcanic Eruption. *Geophysical Research Letters*, 50(4), e2022GL102315. https://doi.org/10.1029/2022GL102315

Manney, G. L., Santee, M. L., Lambert, A., Millan, L., Minschwaner, K., Werner, F., ... & Wang, T. (2023). Siege of the South: Hunga Tonga-Hunga Ha'apai Water Vapor Excluded from 2022 Antarctic Stratospheric Polar Vortex. *Authorea Preprints*. 10.22541/essoar.168057560.00140372/v1

McLinden, C. A., Olsen, S. C., Hannegan, B., Wild, O., Prather, M. J., & Sundet, J. (2000). Stratospheric ozone in 3-D models: A simple chemistry and the cross-tropopause flux. *Journal of Geophysical Research*, 105(D11), 14653–14665. https://doi.org/10.1029/2000JD900124

Mills, M. J., Langford, A. O., O'Leary, T. J., Arpag, K., Miller, H. L., Proffitt, M. H., ... & Solomon, S. (1993). On the relationship between stratospheric aerosols and nitrogen dioxide. *Geophysical research letters*, 20(12), 1187-1190. https://doi.org/10.1029/93GL01124

Mills, M. J., Schmidt, A., Easter, R., Solomon, S., Kinnison, D. E., Ghan, S. J., ... & Gettelman, A. (2016). Global volcanic aerosol properties derived from emissions, 1990–2014, using

CESM1 (WACCM). *Journal of Geophysical Research: Atmospheres*, 121(5), 2332-2348. https://doi.org/10.1002/2015JD024290

Mills, M. J., Richter, J. H., Tilmes, S., Kravitz, B., MacMartin, D. G., Glanville, A. A., ... & Kinnison, D. E. (2017). Radiative and chemical response to interactive stratospheric sulfate aerosols in fully coupled CESM1 (WACCM). *Journal of Geophysical Research: Atmospheres*, 122(23), 13-061. https://doi.org/10.1002/2017JD027006

Millan, L., Santee, M. L., Lambert, A., Livesey, N. J., Werner, F., Schwartz, M. J., ... & Froidevaux, L. (2022). The Hunga Tonga-Hunga Ha'apai hydration of the stratosphere. *Geophysical Research Letters*, 49(13), e2022GL099381. https://doi.org/10.1029/2022GL099381

Murtagh, D., Frisk, U., Merino, F., Ridal, M., Jonsson, A., Stegman, J., Witt, G., Eriksson, P., Jiménez, C., Megie, G., Noë, J. d. l., Ricaud, P., Baron, P., Pardo, J. R., Hauchcorne, A., Llewellyn, E. J., Degenstein, D. A., Gattinger, R. L., Lloyd, N. D., Evans, W. F., McDade, I. C., Haley, C. S., Sioris, C., Savigny, C. v., Solheim, B. H., McConnell, J. C., Strong, K., Richardson, E. H., Leppelmeier, G. W., Kyrölä, E., Auvinen, H., and Oikarinen, L.: An overview of the Odin atmospheric mission, *Can. J. Phys.*, 80, 309–319, https://doi.org/10.1139/p01-157, 2002.

Park, M., Randel, W. J., Kinnison, D. E., Bourassa, A. E., Degenstein, D. A., Roth, C. Z., ... & Santee, M. L. (2017). Variability of stratospheric reactive nitrogen and ozone related to the QBO. *Journal of Geophysical Research: Atmospheres*, 122(18), 10-103. https://doi.org/10.1002/2017JD027061

Portmann, R. W., Solomon, S., Garcia, R. R., Thomason, L. W., Poole, L. R., & McCormick, M. P. (1996). Role of aerosol variations in anthropogenic ozone depletion in the polar regions. *Journal of Geophysical Research: Atmospheres*, 101(D17), 22991-23006. https://doi.org/10.1029/96JD02608

Prather, M., & Jaffe, A. H. (1990). Global impact of the Antarctic ozone hole: Chemical propagation. *Journal of Geophysical Research,* 95(D4), 3473–3492. https://doi.org/10.1029/JD095iD04p03473

Proud, S. R., Prata, A. T., & Schmauß, S. (2022). The January 2022 eruption of Hunga Tonga-Hunga Ha'apai volcano reached the mesosphere. *Science*, 378(6619), 554-557. DOI: 10.1126/science.abo4076

Randel, W. J., Johnston, B. R., Braun, J. J., Sokolovskiy, S., Vömel, H., Podglajen, A., & Legras, B. (2023). Stratospheric Water Vapor from the Hunga Tonga–Hunga Ha'apai Volcanic Eruption Deduced from COSMIC-2 Radio Occultation. *Remote Sensing*, 15(8), 2167. https://doi.org/10.3390/rs15082167

Read, W. G., Froidevaux, L., & Waters, J. W. (1993). Microwave limb sounder measurement of stratospheric SO2 from the Mt. Pinatubo Volcano. *Geophysical Research Letters*, 20(12), 1299-1302. https://doi.org/10.1029/93GL00831

Santee, M. L., Lambert, A., Froidevaux, L., Manney, G. L., Schwartz, M. J., Millan, L., ... & Fuller, R. A. (2023). Strong Evidence of Heterogeneous Processing on Stratospheric Sulfate Aerosol in the Extrapolar Southern Hemisphere Following the 2022 Hunga Tonga-Hunga Ha'apai Eruption. *Authorea Preprints*. DOI: 10.22541/essoar.168500358.84889871/v1

Schoeberl, M. R., Wang, Y., Ueyama, R., Taha, G., Jensen, E., & Yu, W. (2022). Analysis and impact of the Hunga Tonga-Hunga Ha'apai stratospheric water vapor plume. *Geophysical Research Letters*, 49(20), e2022GL100248. https://doi.org/10.1029/2022GL100248

Stimpfle, R. M., Koplow, J. P., Cohen, R. C., Kohn, D. W., Wennberg, P. O., Judah, D. M., ... & Chan, K. R. (1994). The response of ClO radical concentrations to variations in NO2 radical concentrations in the lower stratosphere. *Geophysical research letters*, 21(23), 2543-2546. https://doi.org/10.1029/94GL02373

Stone, K. A., Solomon, S., Kinnison, D. E., Pitts, M. C., Poole, L. R., Mills, M. J., ... & Hagiya, S. (2017). Observing the impact of Calbuco volcanic aerosols on South Polar ozone depletion in 2015. *Journal of Geophysical Research: Atmospheres*, 122(21), 11-862. https://doi.org/10.1002/2017JD026987

Solomon, S., Portmann, R. W., Garcia, R. R., Thomason, L. W., Poole, L. R., & McCormick, M. P. (1996). The role of aerosol variations in anthropogenic ozone depletion at northern midlatitudes. *Journal of Geophysical Research: Atmospheres*, 101(D3), 6713-6727. https://doi.org/10.1029/95JD03353

Solomon, S., Borrmann, S., Garcia, R. R., Portmann, R., Thomason, L., Poole, L. R., ... & McCormick, M. P. (1997). Heterogeneous chlorine chemistry in the tropopause region. *Journal of Geophysical Research: Atmospheres*, 102(D17), 21411-21429. https://doi.org/10.1029/97JD01525

Solomon, S., Portmann, R. W., Garcia, R. R., Randel, W., Wu, F., Nagatani, R., ... & McCormick, M. P. (1998). Ozone depletion at mid-latitudes: Coupling of volcanic aerosols and temperature variability to anthropogenic chlorine. *Geophysical Research Letters*, 25(11), 1871-1874. https://doi.org/10.1029/98GL01293

Solomon, S. (1999). Stratospheric ozone depletion: A review of concepts and history. *Reviews of geophysics*, 37(3), 275-316. https://doi.org/10.1029/1999RG900008

Solomon, S., Portmann, R. W., Sasaki, T., Hofmann, D. J., & Thompson, D. W. (2005). Four decades of ozonesonde measurements over Antarctica. *Journal of Geophysical Research: Atmospheres*, 110(D21). https://doi.org/10.1029/2005JD005917

Solomon, S., Kinnison, D., Bandoro, J., & Garcia, R. (2015). Simulation of polar ozone depletion: An update. *Journal of Geophysical Research: Atmospheres*, 120(15), 7958-7974. https://doi.org/10.1002/2015JD023365

Solomon, S., Ivy, D. J., Kinnison, D., Mills, M. J., Neely III, R. R., & Schmidt, A. (2016). Emergence of healing in the Antarctic ozone layer. *Science*, 353(6296), 269-274. DOI: 10.1126/science.aae0061

Stone, K. A., Solomon, S., Kinnison, D. E., Pitts, M. C., Poole, L. R., Mills, M. J., ... & Hagiya, S. (2017). Observing the impact of Calbuco volcanic aerosols on South Polar ozone depletion in 2015. *Journal of Geophysical Research: Atmospheres*, 122(21), 11-862. https://doi.org/10.1002/2017JD026987

Taha, G., Loughman, R., Colarco, P. R., Zhu, T., Thomason, L. W., & Jaross, G. (2022). Tracking the 2022 Hunga Tonga-Hunga Ha'apai aerosol cloud in the upper and middle stratosphere using space-based observations. *Geophysical Research Letters*, 49(19), e2022GL100091. https://doi.org/10.1029/2022GL100091

Tie, X., & Brasseur, G. (1995). The response of stratospheric ozone to volcanic eruptions: Sensitivity to atmospheric chlorine loading. *Geophysical Research Letters*, 22(22), 3035-3038. https://doi.org/10.1029/95GL03057

Vömel, H., Evan, S., & Tully, M. (2022). Water vapor injection into the stratosphere by Hunga Tonga-Hunga Ha'apai. *Science*, 377(6613), 1444-1447. DOI: 10.1126/science.abq2299

Wang, X., Randel, W., Zhu, Y., Tilmes, S., Starr, J., Yu, W., ... & Li, J. (2022). Stratospheric climate anomalies and ozone loss caused by the Hunga Tonga volcanic eruption. *Authorea Preprints*. DOI: 10.1002/essoar.10512922.1

Wennberg, P. O., Cohen, R. C., Stimpfle, R. M., Koplow, J. P., Anderson, J. G., Salawitch, R. J., ... & Wofsy, S. C. (1994). Removal of stratospheric O3 by radicals: In situ measurements of OH, HO2, NO, NO2, ClO, and BrO. *Science*, 266(5184), 398-404. DOI: 10.1126/science.266.5184.398

Xu, J., Li, D., Bai, Z., Tao, M., & Bian, J. (2022). Large amounts of water vapor were injected into the stratosphere by the hunga tonga–hunga ha'apai volcano eruption. *Atmosphere*, 13(6), 912. https://doi.org/10.3390/atmos13060912

Zambri, B., LeGrande, A. N., Robock, A., & Slawinska, J. (2017). Northern Hemisphere winter warming and summer monsoon reduction after volcanic eruptions over the last millennium. *Journal of Geophysical Research: Atmospheres*, 122(15), 7971-7989. https://doi.org/10.1002/2017JD026728

Zambri, B., Solomon, S., Kinnison, D. E., Mills, M. J., Schmidt, A., Neely III, R. R., ... & Roth, C. Z. (2019). Modeled and observed volcanic aerosol control on stratospheric NOy and

Cly. *Journal of Geophysical Research: Atmospheres*, 124(17-18), 10283-10303. https://doi.org/10.1029/2019JD031111

Zhang, J., Wuebbles, D., Kinnison, D., & Baughcum, S. L. (2021). Stratospheric ozone and climate forcing sensitivity to cruise altitudes for fleets of potential supersonic transport aircraft. *Journal of Geophysical Research: Atmospheres,* 126(16), e2021JD034971. https://doi.org/10.1029/2021JD034971

Zhu, Y., Toon, O. B., Kinnison, D., Harvey, V. L., Mills, M. J., Bardeen, C. G., ... & Jégou, F. (2018). Stratospheric aerosols, polar stratospheric clouds, and polar ozone depletion after the Mount Calbuco eruption in 2015. *Journal of Geophysical Research: Atmospheres*, 123(21), 12-308. https://doi.org/10.1029/2018JD028974

Zhu, Y., Bardeen, C. G., Tilmes, S., Mills, M. J., Wang, X., Harvey, V. L., ... & Toon, O. B. (2022). Perturbations in stratospheric aerosol evolution due to the water-rich plume of the 2022 Hunga-Tonga eruption. *Communications Earth & Environment*, 3(1), 248. https://doi.org/10.1038/s43247-022-00580-w

Chemistry contribution to stratospheric ozone depletion after the unprecedented water rich Hunga Tonga eruption

Authors: Jun Zhang[1*], Douglas Kinnison[1], Yunqian Zhu[2,3], Xinyue Wang[1], Simone Tilmes[1], Kimberlee Dube[4], William Randel[1]

Affiliations:

[1]Atmospheric Chemistry Observations & Modeling Laboratory, National Center for Atmospheric Research, Boulder, CO, USA

[2] Cooperative Institute for Research in Environmental Sciences, University of Colorado Boulder, Boulder, CO, USA, 80309

[3]Chemical Sciences Laboratory, National Oceanic and Atmospheric Administration, Boulder, CO, USA, 80305

[4]Institute of Space and Atmospheric Studies, University of Saskatchewan, Saskatoon, SK, Canada

[*]Corresponding author: Jun Zhang (jzhan166@ucar.edu)

Key Points:

- Nudged chemistry-climate model simulations are used to quantify the chemistry impact on the stratospheric ozone following the Hunga Tonga-Hunga Ha'apai eruption.
- The modeled ozone and nitrogen oxides anomalies show a good agreement with satellite observations.
- Chemistry contributes to 6% and 20% ozone depletion at mid-latitudes and Antarctica, respectively.

Abstract

Following the Hunga Tonga–Hunga Ha'apai (HTHH) eruption in January 2022, stratospheric ozone depletion was observed in the Southern Hemisphere mid-latitudes and Antarctica during the 2022 austral wintertime and springtime. This eruption injected sulfur dioxide and unprecedented amounts of water vapor into the stratosphere. This work examines and quantifies the chemistry contribution of the volcanic materials to the ozone depletion using chemistry-climate model simulations with nudged meteorology. Simulated 2022 ozone and nitrogen oxides (NO_x) anomalies show a good agreement with satellite observations. We find that chemistry only contributes up to 6% and 20% ozone destruction at mid-latitudes wintertime and Antarctic springtime respectively. The majority of the ozone depletion is attributed to the internal variability and dynamical changes forced by the eruption. Both the simulation and observations show a significant NOx reduction associated with the HTHH aerosol plume, indicating the enhanced dinitrogen pentoxide hydrolysis on sulfate aerosol.

Plain language summary

The January 2022 eruption of the Hunga Tonga-Hunga Ha'apai underwater volcano injected a large amount of water vapor (H_2O) and moderate amounts of sulfur dioxide (SO_2) into the stratosphere. Stratospheric ozone losses were observed following the eruption in the Southern Hemisphere (SH) mid-latitudes and Antarctica during the 2022 austral wintertime and springtime. The ozone layer in the stratosphere protects Earth's human being and biosphere from harmful ultraviolet light by absorbing the harmful portion of the radiation from the sun. We use computer simulation in this study to examine the impacts of chemical processes on the ozone layer from the volcanic materials. We find that chemistry is contributing up to 6% and 20% of the ozone reduction at SH mid-latitudes winter and Antarctic spring respectively. The majority of ozone changes are due to transport and dynamical processes from internal variability in the climate system and forced response by the HTHH eruption.

1. Introduction

It has been long known that explosive volcanic eruptions can cause stratospheric ozone depletion by injecting sulfate and its precursor SO_2 into the stratosphere, which enhances aerosol surface areas for heterogeneous chemistry (Hofmann & Solomon, 1989; Portmann et al., 1996; Kinnison et al., 1994; Solomon et al., 1996, 1998). Observations have shown that Antarctic ozone depletion was enhanced after the major eruption of Mount Pinatubo in the early 1990s with injections of ~18 Tg sulfur dioxide (SO_2) (e.g., Read et al., 1993; Krueger et al., 1995; Solomon et al., 2005). Even the moderate magnitude volcanic eruption of Calbuco in 2015, which injected 0.4 Tg of SO_2, exacerbated ozone depletion, producing a record-breaking October ozone hole that lasted late into the season (Solomon et al., 2016; Ivy et al., 2017; Stone et al., 2017; Zhu et al., 2018).

The January 2022 Hunga Tonga–Hunga Ha'apai (HTHH) eruption was an unprecedented underwater volcanic event of the modern era, which injected volcanic materials to altitudes up to 58 km in the mesosphere (Carr et al., 2022; Proud et al., 2022). Unlike land-based volcanoes such as Mount Pinatubo and Calbuco, HTHH injected about 150 Tg of water (H_2O) (Xu et al., 2022; Millán et al., 2022) along with 0.4 to 0.5 Tg SO_2 into the stratosphere (Carn et al. 2022; Taha et al., 2022). This H_2O injection increased the global stratospheric water burden by more than 10% (Vömel et al., 2022; Khaykin et al., 2022; Randel et al., 2023). The additional source of H_2O can impact the ozone chemistry by altering the HOx chemical cycles, heterogeneous reaction rate, and the Polar Stratospheric Cloud formation (PSCs) (Solomon et al., 1997; Anderson et al., 2012). In addition, volcanic aerosols provide extra surface area density (SAD) for heterogeneous reactions affecting ozone chemistry, and suppressing the NOx-Ox cycles (defined later in Section 3.2) (Tie and Brasseur, 1995).

Previous studies have utilized the chemistry-climate model Community Earth System Model Version 2 (CESM2) with Whole Atmosphere Community Climate Model Version 6 (WACCM6) to simulate the dispersion and evolution of aerosol and water plumes after the HTHH eruption (Zhu et al., 2022; Wang et al., 2023, Lu et al., 2023). WACCM6 simulations reproduced the Microwave Limb Sounder (MLS) observed evolution of the H_2O throughout 2022 and the stratospheric cooling and circulation changes as seen by European Center for Medium Range Forecasts ERA5 reanalysis (Wang et al., 2023). Zhu et al. (2022) found that the additional water

vapor increases hydroxide, halves the sulfur dioxide lifetime, promotes faster sulfate aerosol formation as seen by Cloud-Aerosol Lidar and Infrared Pathfinder Satellite Observation (CALIPSO) and The Ozone Mapping and Profiler Suite Limb Profiler (OMPS-LP), and leads to the increased aerosol optical depth and radiation effect. The persistent perturbations in H_2O and aerosol due to HTHH plumes in the SH stratosphere throughout 2022 draw attention to exploring the SH stratospheric ozone response.

Lu et al. (2023) explored the ozone response to the HTHH eruption considering 0.4 Tg SO_2 emission but ignored the large H_2O injection. Wang et al. (2023) simulated large stratospheric ozone anomalies in mid-latitudes and Antarctica in 2022 as observed by MLS. Manney et al. (2023) looked into the nitrous oxide anomalies with ozone and suggested that transport plays a role in the ozone reduction. However, the relative effects of chemistry and dynamics on these ozone anomalies has not been quantified. This work aims to examine and quantify the chemical ozone depletion and the associated chemical processes in the wake of HTHH. We isolate the ozone impact owing to chemistry by nudging the model dynamics to meteorology analysis fields.

2. Data and Model

2.1 Microwave Limb Sounder (MLS)

The MLS instrument was launched on NASA's EOS Aura satellite on July 15, 2004. For the past 19 years, MLS has provided a uniquely comprehensive suite of daily global measurements for studying lower stratospheric chemical processing. MLS Version 5.0 data is used in this work. The standard product for O_3 is derived from MLS radiance measurements near 240 GHz; the O_3 data and its validation are described by Livesey et al. (2020). The useful data range is from 261 hPa up to 0.001 hPa. Here the O_3 data used are compiled into a daily zonal means at a resolution of 2.5° latitude from 2004 to 2022. Anomalies for 2022 shown in this study are calculated based on climatology background from 2007 to 2021, as the model simulations started from 2007.

2.2 Optical Spectrograph and InfraRed Imager System (OSIRIS)

The Optical Spectrograph and InfraRed Imager System (OSIRIS) has been in sun-synchronous orbit on the Odin satellite since 2001 (Llewellyn et al., 2004; Murtagh et al., 2002). The optical spectrograph scans the atmospheric limb to measure vertical profiles of limb-scattered solar irradiance between 275 and 810 nm. There are between 100 and 400 profiles per day, depending on the time of year and the scanning range. Only the descending node measurements are considered here due to a drift in the orbit that has caused inconsistent ascending node sampling over the course of the mission. We use NOx from version 7.2 of the OSIRIS retrieval, which is described and validated in Dubé et al. (2022). The OSIRIS NO_2 observations are converted to NOx using the PRATMO photochemical box model (Prather and Jaffe, 1990; McLinden et al., 2000), following the process in Dubé et al. (2020). PRATMO is also used to scale the OSIRIS measurements to a common local solar time of 12:00 pm in order to account for variations in the measurement time caused by the processing satellite orbit, which is described in Dubé et al. (2020).

2.3 Whole Atmosphere Community Climate Model (WACCM)

The CESM2/WACCM6 was used to conduct the numerical experiments. This state-of-the-art chemistry-climate model extends from the Earth's surface to approximately 140 km and includes comprehensive troposphere-stratosphere-mesosphere-lower-thermosphere (TSMLT) chemistry (details described in Gettelman et al., 2019). WACCM6 includes a prognostic stratospheric aerosol

module (Mills et al., 2016) and has been utilized extensively to study volcanic aerosols and their impact on climate change and ozone losses (e.g., Mills et al., 2017; Stone et al., 2017; Zambri et al., 2019). In this study, the simulations feature a horizontal resolution of 0.9° latitude × 1.25° longitude using the finite volume dynamical core (Lin & Rood, 1996), and 110 vertical levels, with a vertical resolution of ~500m in the upper troposphere and lower stratosphere. WACCM6 is run in a specified dynamics configuration (WACCM6-SD), where the temperatures and winds are relaxed to Modern-Era Retrospective analysis for Research and Applications Version 2 (MERRA-2) reanalyses (Gelaro et al., 2017) using a relaxation time of 50 hours. This configuration starts from 2007 until the end of 2022, using initial conditions from a long historical simulation (Gettelman et al., 2019). Starting in January 2022, we conduct two cases: the experiment case with full forcing (SO_2 and H_2O injection) from the HTHH eruption (as defined in Zhu et al., 2022) and the control case with no forcing (no SO_2 or H_2O injection) from HTHH eruption. The difference between these two nudged simulations gives information about the chemistry contribution to the stratospheric ozone depletion after the HTHH eruption. We use the emission described in Zhu et al. (2022), where 150 Tg of H_2O and 0.42 Tg of SO_2 are injected on January 15, 2022, from ~20 to 35 km.

3. Results and Discussions

3.1 Observed and simulated ozone anomaly from MLS and WACCM6-SD

It is expected that the large HTHH H_2O and aerosol perturbations can impact stratospheric dynamics and chemistry, and hence ozone abundances. Figure 1 shows MLS observed ozone from 2004 to 2022 and WACCM6-SD simulated ozone during 2022 in the stratosphere. MLS satellite observations indicate anomalous negative ozone in 2022 both over SH midlatitudes and tropics (10°S-60°S) in winter as well as Antarctica (60°S-82°S) in spring. The MLS ozone concentration over 10°S-60°S shows a record low relative to the climatology period (2004 to 2022) in the SH austral winter (Fig. 1a, red line) at 30 hPa. Large midwinter interannual variability in this region is linked to the Quasi-Biennial Oscillation (QBO), as discussed in Wang et al. (2023). MLS also shows a relatively deep ozone hole in the SH austral spring (Fig. 1b) at 80 hPa. The negative ozone anomaly over the polar region (60°S-82°S) is large in October-December, but within the variability of previous years. This is because the climatology period (2004 to 2022) also includes years with either relatively strong polar vortex or volcanic impact. For example, the lowest line in Figure 1b is in the year 2015, when a record October ozone hole occurred after the Calbuco volcanic eruption (Solomon et al., 2015; Ivy et al., 2017). The accuracy of MLS O_3 is about 0.2 ppmv at 30 hPa and 0.1 ppmv near 80 hPa (Livesey et al., 2020). The difference between MLS climatology mean and 2022 is outside the MLS ozone systematic error during June-August in Fig. 1a and October in Fig. 1b, which reinforces the anomalous low ozone occurring in the SH mid-latitudes winter and Antarctica spring 2022. WACCM6-SD captures both the record low ozone over 10°S-60°S and the large ozone anomaly over 60°S-82°S, and is within the systematic error of MLS, except in December 2022 in Fig. 1b.

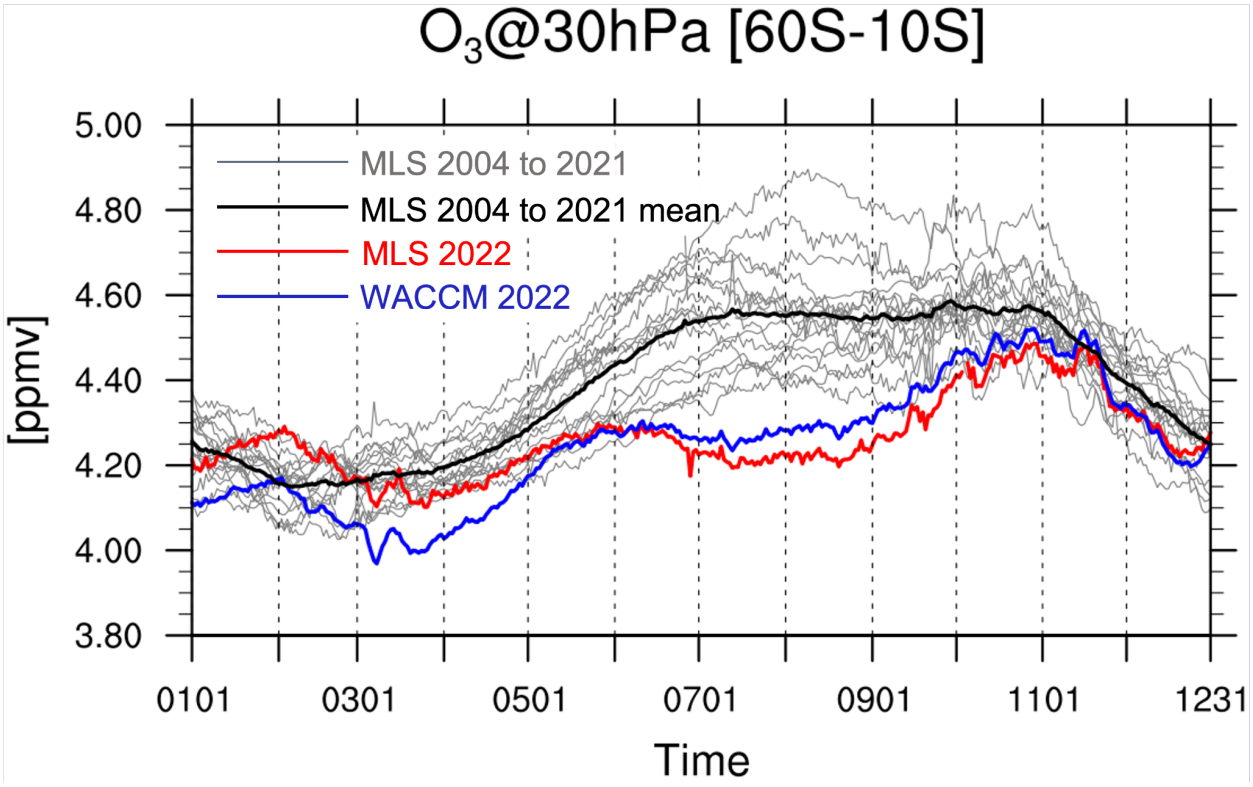
O3@30hPa [60S-10S]
MLS 2004 to 2021
MLS 2004 to 2021 mean
MLS 2022
WACCM 2022
[ppmv]
5.00
4.80
4.60
4.40
4.20
4.00
3.80
0101
0301
0501
0701
0901
1101
1231
Time

(a)

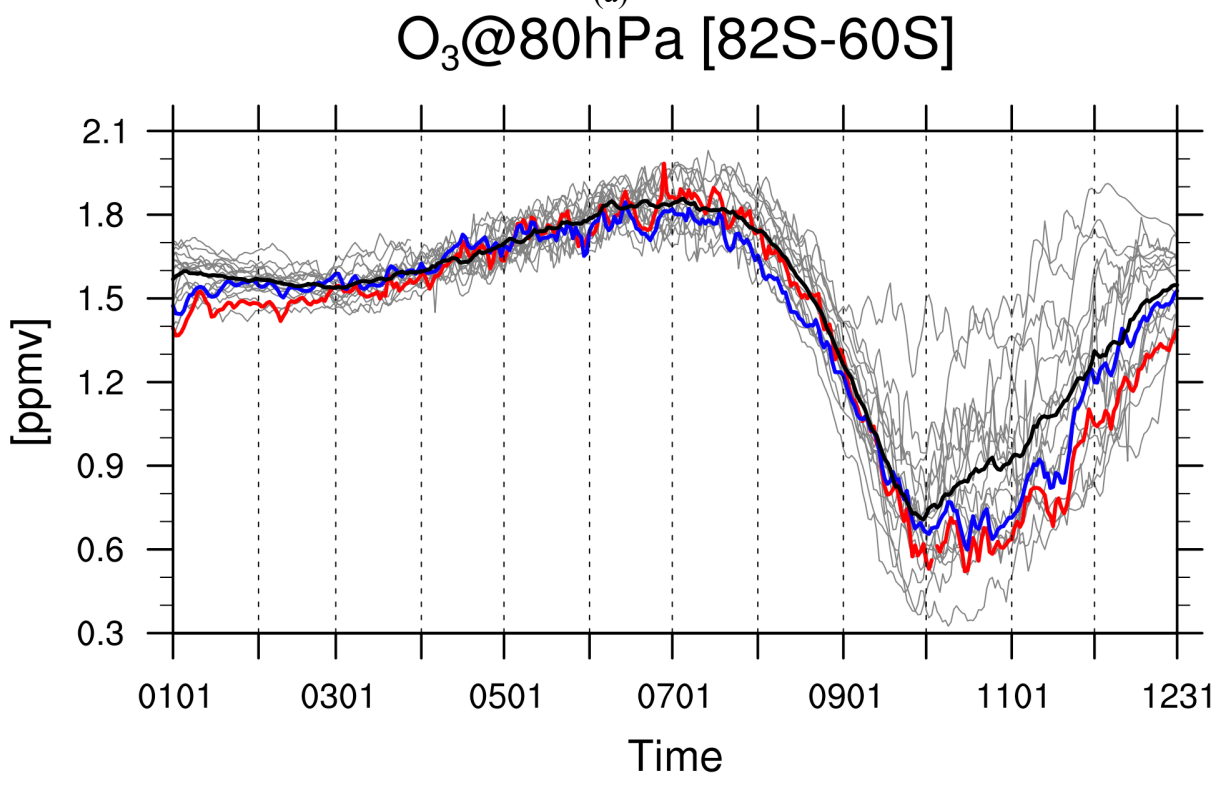
O3@80hPa [82S-60S]
[ppmv]
2.1
1.8
1.5
1.2
0.9
0.6
0.3
0101
0301
0501
0701
0901
1101
1231
Time

(b)

Figure 1. Time series of ozone concentration (ppmv) for (a) midlatitudes and tropics (10°S-60°S) at 30 hPa and (b) polar region (60°S-82°S) at 80 hPa from MLS and WACCM. MLS observations are shown from 2004 to 2022. Gray lines show time serieses of MLS ozone during 2004-2021 and the black line indicates the mean MLS ozone over the climatology. The red and blue lines are for MLS and WACCM6-SD ozone in 2022, respectively.

3.2 Quantifying the chemical contribution to the ozone reduction

Stratospheric ozone changes in 2022 compared with the climatology can be attributed to various factors: internal variability in the climate system (e.g., QBO), and forced changes after the HTHH eruption including both dynamics and chemistry impacts. Both observed and simulated 2022 anomalies showing in the following are calculated as deviations from the 2007-2021 background instead of 2004-2021 to be consistent with model simulation period. We note that the difference of the derived 2022 anomaly between using 2004 and 2007 is minimal. The derived ozone anomaly from MLS and WACCM6-SD in August are shown in Figure 2a and 2b. The lower stratospheric wintertime SH mid-latitude ozone reduction is well represented in WACCM6-SD, along with the ozone increase in the tropics, which is related to the QBO. These ozone anomalies are the result of the combination of internal variability and HTHH eruption forced changes. Figure 2c shows the ozone changes due to chemistry only, calculated by taking the difference between the full forcing experiment run (SO_2+H_2O) and the no forcing control run in 2022. The blue and red contour lines highlight the location of HTHH water and aerosol plumes, which reveals the separation of the H_2O and aerosol plumes over time due to the sedimentation of the aerosols (Legras et al. 2022, Wang et al., 2023). As the experiment and control simulations are nudged to the same dynamics, the ozone changes in Figure 2c are purely due to the chemistry impact from the enhanced water and aerosol SAD perturbation. The ozone depletion over the SH mid-latitudes ranges from 200 hPa up to 30 hPa. In particular, the reduction at 30 to 50 hPa and 100 to 200 hPa are outside of previous variability (hatched region), with the peak reaching about 20% ozone reduction. Chemistry only contributes up to 6% of ozone depletion at mid-latitudes near 70 hPa (Fig. 2c). Consequently, less than 30% of the ozone reduction at the hatched regions in Figure 2a and 2b is attributed to chemistry, with the other changes a result of dynamical changes due to internal variability from QBO and forced dynamical response to the HTHH eruption.

In the springtime (October-December) of the Antarctic polar region, a large negative ozone anomaly is observed within the polar vortex (south of 60˚S) in 2022 (Fig. 2d), even though it is not a record-breaking low ozone hole (not hatched). WACCM6-SD reproduces this large ozone reduction in general, but slightly underestimates the ozone loss between 30 to 50 hPa (Fig. 2e). The simulation (Fig. 2f) shows that the aerosol plume from the HTHH eruption entered the Antarctic near the bottom of the polar vortex (~100 hPa) in October. However, the water plume was confined outside of the polar vortex due to the strong polar jet stream near 25 km (Schoeberl et al. 2023; Manney et al, 2023; Wang et al., 2023). Note that although the simulated HTHH aerosol penetrated across the bottom of the polar vortex, it is difficult to prove it with observations. Enhanced polar extinction in OMPS-LP measurements can be due to polar stratospheric clouds in the winter season (Manney et al., 2023; Wang et al., 2023). In addition, the amount of sulfate entering the polar vortex in the simulation is relatively small (only double the background), and satellite observations (e.g., CALIPSO lidar) sometimes cannot capture it due to background noise

level. The ozone depletion simulated in Figure 2f is because the volcanic aerosol entered the bottom of the polar vortex which provides additional SAD for heterogeneous chemistry in the polar region. Chemistry (Fig. 2f) leads to ~ 20% ozone reduction (this is equivalent to about 40% of the total ozone depletion) near the center of the Antarctic vortex.

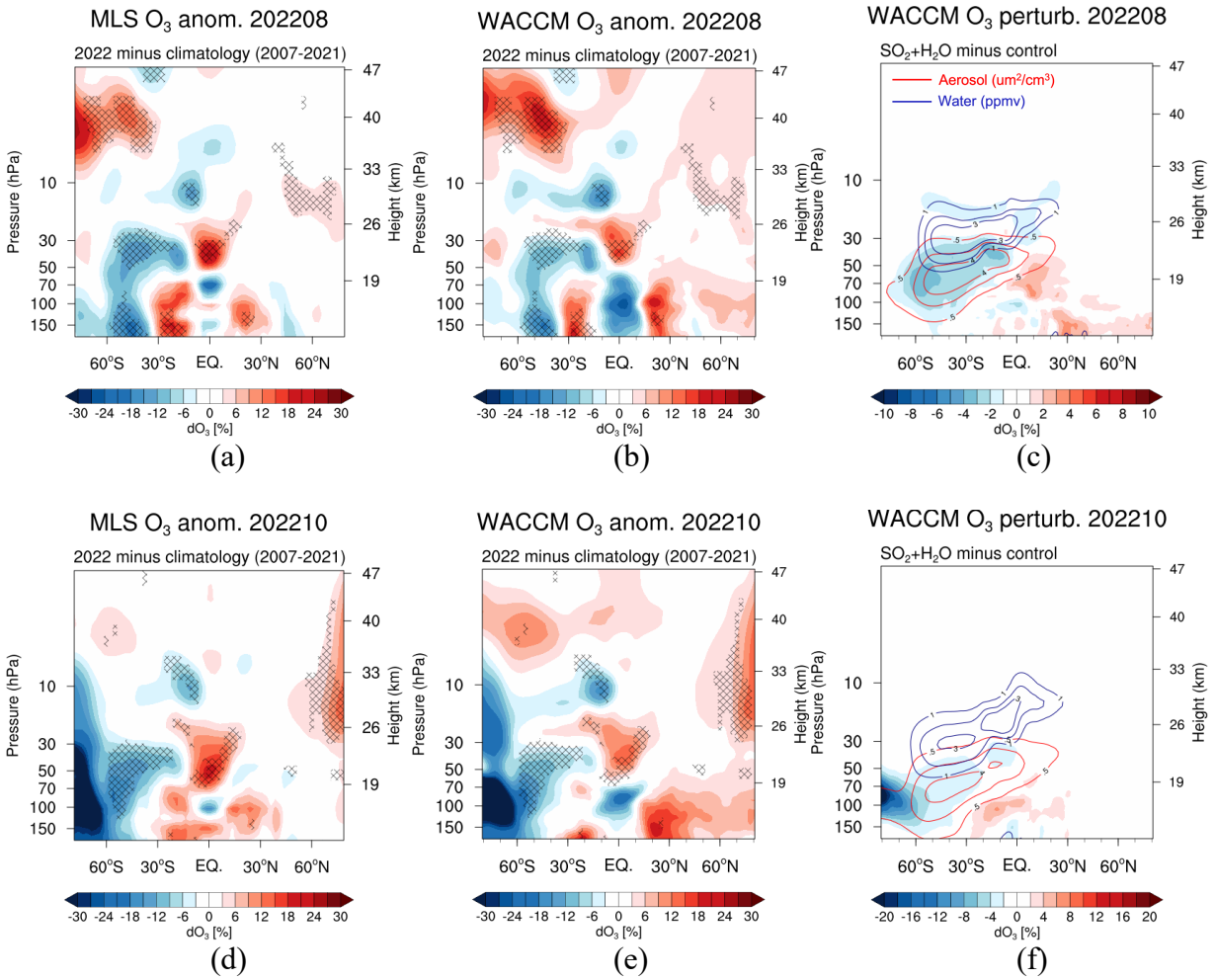

Figure 2. Percentage change of 2022 ozone anomaly (%) relative to climatology (2007 to 2021) from MLS (a) and WACCM6-SD (b) in August. (d) and (e) are the same but for October. Hatched regions indicate where the 2022 anomalies are outside the range of all variability during 2007-2021. Percentage change of ozone (%) calculated from full-forcing (SO_2+H_2O) compared to no-forcing control runs in August (c) and October (f). The blue and red contour lines in (c) and (f) are water anomaly in ppmv and aerosol surface area density anomaly in um^2/cm^3, respectively. Note that panel c and f have different color bar ranges from panel a, b, d, e.

We characterize the major chemical processes that lead to the 6% and 20% of chemical ozone depletion in the mid-latitudes and polar regions discussed above. The chemical destruction of odd oxygen (Ox = O_3 + O + $O(^1D)$ + other terms; Brasseur & Solomon, 2005) is directly linked to ozone abundance in the stratosphere. Different Ox catalytic destruction cycles involve nitrogen oxides (NOx-Ox), hydrogen radicals (HOx-Ox), halogen oxides (ClOx/BrOx-Ox) as well as the chemical loss by the Chapman self-destruction mechanism (Ox-Ox) (e.g., Crutzen & Ehhalt, 1977;

Solomon, 1999). Supplementary Text S1 defines the odd oxygen used in this study and the reactions that are contained in each odd oxygen chemical family. Figure 3a and 3b characterize the total Ox loss (sum of Ox-Ox, NOx-Ox, HOx-Ox and ClOx/BrOx-Ox cycles) during the SH winter and spring. The changes in Ox are induced by the addition of water and aerosol injection from HTHH eruption. In the wintertime, the major Ox loss occurs in the mid-latitudes from 150 to 20 hPa, consistent with the location of major ozone loss in Figure 2c. During springtime, the total Ox loss extends into the polar region, associated with the aerosol plume shown in Figure 2f.

The vertical profile of changes in individual loss cycles are illustrated in Figure 3c and 3d for mid-latitudes winter and Antarctic spring, respectively. Increasing aerosol surface areas decrease the abundance of NOx and hence the NOx-catalyzed ozone destruction cycles (red lines) (discussed in section 3.3). Both HOx-Ox and ClOx/BrOx-Ox cycles play important roles in the chemical ozone destruction for mid-latitudes winter, but at different altitudes. The HOx-Ox cycle is more significant at 20 to 30 km, while the ClOx/BrOx-Ox cycle plays a larger role below 20 km. The enhanced HOx cycle is the combined results of direct water injection and the HOx repartitioning induced from NOx reduction (Wennberg et al., 1994; Solomon et al., 1996). The reduced NOx also gives rise to ClOx enhancement as ClOx is inversely correlated with NOx (Stimpfle et al., 1994; Solomon et al., 1999). In the Antarctic spring, ClOx/BrOx-Ox cycle controls the behavior of total Ox change below around 18 km. HOx-Ox loss cycle is still the major loss mechanism at 20 to 25 km. However, this loss is largely offset by hindered NOx-Ox loss, which is normally the most important loss cycle at this altitude in the background atmosphere (Zhang et al., 2021). It is eye-catching to see there is a negative Ox perturbation at around 16-18 km, corresponding to 70-100 hPa in Figure 2b. This is because the ozone abundances in the experiment run drop to extreme low values at 70-100 hPa in the core of the vortex, hence the formation of ClO (and therefore chlorine nitrate $ClONO_2$) is impeded (Fig. S1). Rapid deactivation of Cl into hydrochloric acid (HCl) then occurs even if the enhanced SAD are still present and temperatures are very cold (Douglass et al., 1995; Solomon et al., 2015). This rapid deactivation suppresses the Ox loss due to ClOx/BrOx-Ox cycle in the experiment run compared to the control run. Figure 3c and 3d indicate that the reaction rates of all the Ox chemical loss cycles are modified even though only SO_2 and H_2O emissions are injected into the atmosphere from the HTHH eruption. This is expected since these cycles couple to each other and change repartitioning from each other.

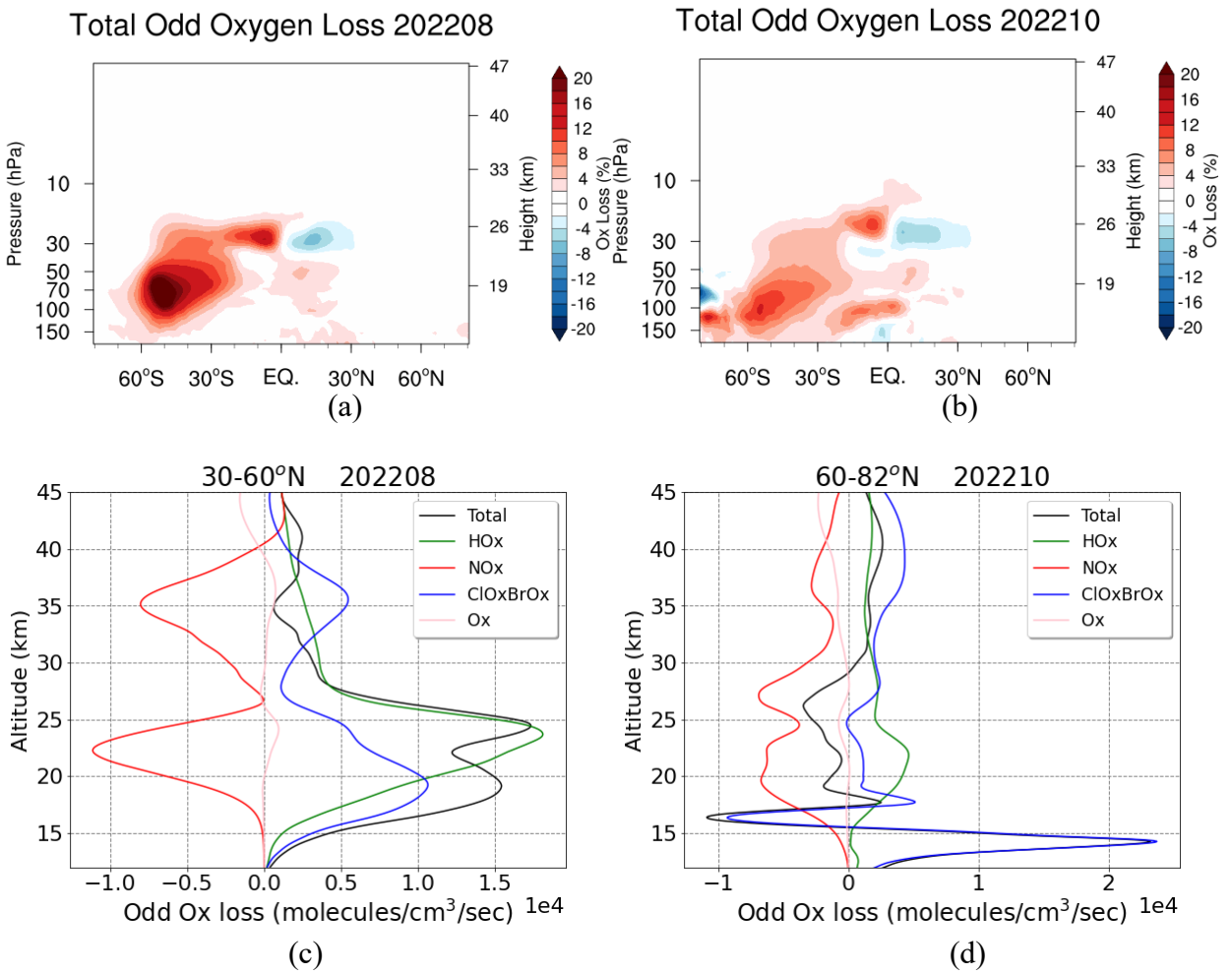

Figure 3. Calculated perturbations from full-forcing (SO_2+H_2O) experiment run compared to no-forcing control run for total OddOx loss in August (a) and October (b). Vertical profile of total Odd oxygen (Ox) loss (in black) and the loss from individual cycles of HOx-Ox, NOx-Ox, ClOxBrOx-Ox and Ox-Ox at mid-latitudes in August (c) and Antarctic region in October (d).

3.3 Negative NOx anomaly after HTHH eruption

NOx reduction is expected following large volcanic eruptions, which perturbs ozone abundance in the stratosphere (e.g., Fahey et al., 1993; Mills et al., 1993; Berthet et al., 2017; Zambri et al., 2019). Figure 4 examines the NOx anomaly after the HTHH eruption from OSIRIS observations and WACCM6-SD model simulations. A dipole pattern is observed both in the OSIRIS and WACCM: a NOx reduction at around 25 km and below, and a positive anomaly above. This positive anomaly is mainly due to the QBO internal variability, as it is also seen in 2008 when the QBO phase is similar to 2022 while the negative anomaly is not found (Fig. S2) (Park et al., 2017). Figure 4a and 4d show the OSIRIS observed NOx anomalies in August and October 2022, with reductions of 30~40% over the mid-latitude lower stratosphere. This negative anomaly is approximately collocated with the HTHH aerosol plume in Figure 2c and 2f, which is consistent with the plume location shown in Wang et al. (2023) from the OMPS-LP data. The HTHH aerosol

reduce the NOx abundance via the well-known heterogeneous chemical reactions dinitrogen pentoxide (N_2O_5) hydrolysis on aerosols (e.g., Hofmann and Solomon, 1989; Solomon, 1999; Berthet et al., 2017). Due to the N_2O_5 hydrolysis on the surface of aerosol, nitric acid (HNO_3) formation is promoted which acts as a major sink of NOx in the atmosphere during night-time. We note that OSIRIS data show strong NOx decreases throughout 2022 (not shown) that overlap the HTHH aerosol layer, but OSIRIS does not have high latitude measurements during midwinter. Model calculations (Fig. 4b and 4e) show NOx decreases in the lower stratosphere that are similar in magnitude (~30-40%) and location to the OSIRIS results, demonstrating that the NOx-aerosol reactions are captured well in the model. Figure 4c and 4f denote the modeled changes in N_2O_5 hydrolysis rate overlying with aerosol SAD anomaly due to the HTHH eruption, derived from the difference between full-forcing (SO_2+H_2O) and no-forcing control runs. This heterogeneous chemical reaction rate is enhanced by more than 50% at the location where the maximum of NOx reduction occurs in Figure 4b and 4e. The results shown here are consistent with the conclusion drawn from Santee et al. (2023) using MLS data, suggesting the hydrolysis of N_2O_5 is the primary mechanism for the reduction of NOx. We note that even though this NOx reduction is significant, we found that the NOx impact on ozone is largely canceled by HOx-Ox and ClOx-Ox cycles as shown in Figure 3c and 3d.

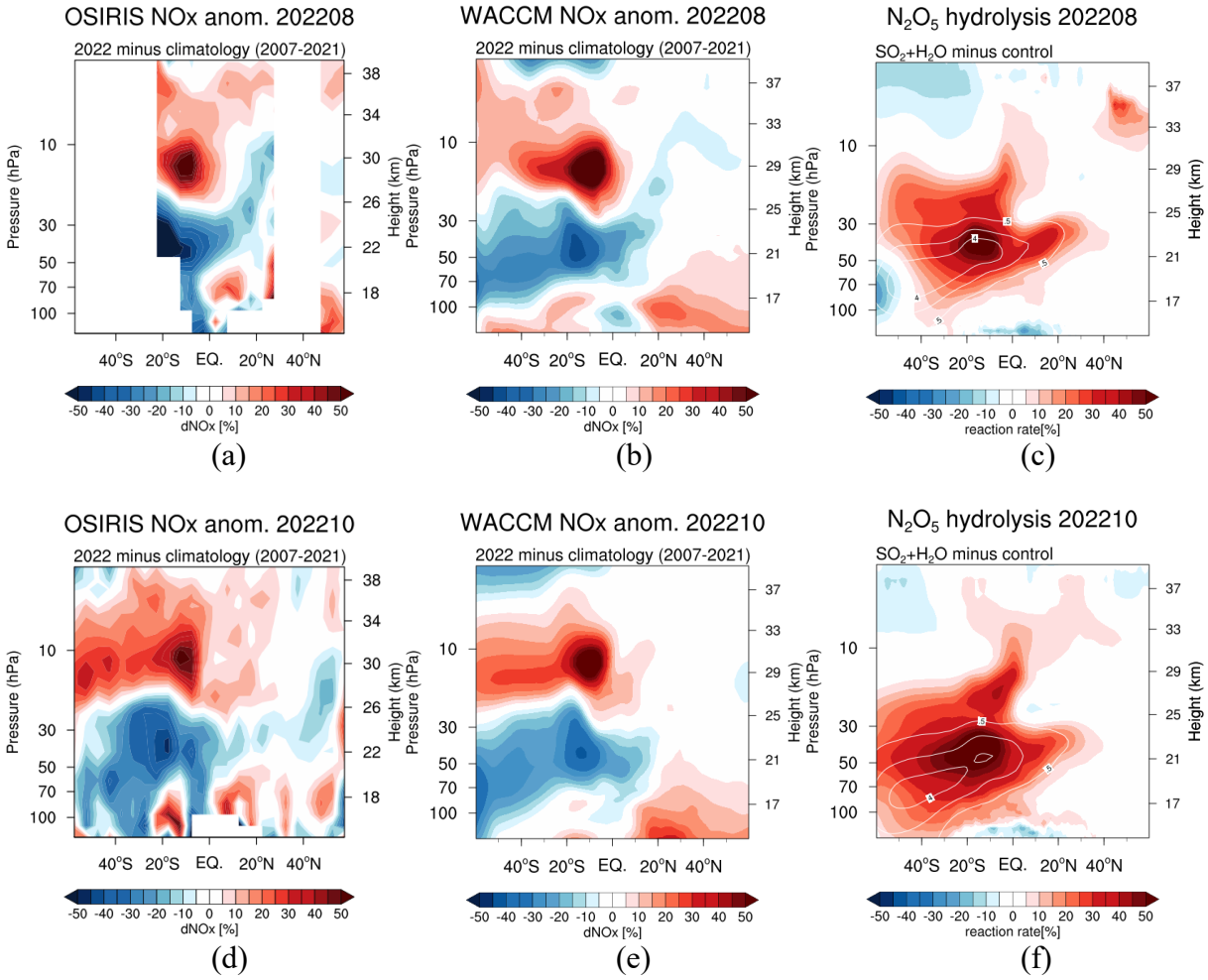

Figure 4. Calculated NOx anomaly (%) relative to climatology (2007 to 2021) from OSIRIS and WACCM6-SD in August and October (a), (b) and (d), (e). Calculated changes (%) in N_2O_5 hydrolysis rate on sulfate aerosols in the WACCM6-SD model from full-forcing (SO_2+H_2O) compared to no-forcing control runs in August and October (c) and (f). The white contour line in (c) and (f) is the aerosol surface area density anomaly in um^2/cm^3.

4. Summary and discussion

The January 2022 Hunga Tonga-Hunga Ha'apai eruption injected ~150 Tg of water and ~0.42 Tg SO_2 into the SH stratosphere. MLS observed ozone reductions in the SH stratosphere mid-latitudes and Antarctica during the 2022 austral wintertime and springtime. This work focuses on examining and quantifying the chemical ozone depletion due to the SO_2 and H_2O injection. We use WACCM6-SD nudged simulations to disentangle the role of chemistry from that of dynamics. WACCM6-SD shows a good agreement with MLS ozone anomaly and also reproduces the NOx anomaly in 2022 compared to OSIRIS measurements.

We found chemistry contributes to 6% and 20% ozone depletion at mid-latitudes and Antarctica, respectively. The majority of ozone changes are due to transport and dynamical processes from internal variability in the climate system and forced response by the HTHH eruption. One caveat is that the chemistry quantified here does not include the dynamics feedback on the chemistry. For example, water can cool the stratosphere, which would further promote heterogeneous reactions. However, because these two simulations conducted here are nudged to the same dynamics, the temperature is not allowed to change to reflect the feedback on chemistry. To characterize the chemical processes that contributed to the ozone loss, different loss cycles (NOx-Ox, HOx-Ox, ClOx/BrOx-Ox and Ox-Ox) were examined and their relative significance to the ozone depletion at SH mid-latitudes and Antarctica were evaluated. We found both HOx-Ox and ClOx/BrOx-Ox cycles play important roles in the total chemical ozone destruction for mid-latitudes winter. While during the Antarctic spring, ClOx/BrOx-Ox cycle is dominant and controls the behavior of total Ox change in the lower stratosphere. We also document that both OSIRIS and WACCM6-SD show a NOx reduction that collocates with HTHH aerosols plume, demonstrating the enhanced N_2O_5 hydrolysis on sulfate aerosol. Consequently, the NOx-Ox loss cycle is strongly suppressed associated with the significant NOx reduction. However, the NOx impact on ozone is minimal since it is largely canceled by HOx-Ox and ClOx/BrOx-Ox cycles.

Acknowledgments

Jun Zhang and Xinyue Wang are supported by the NSF via NCAR's Advanced Study Program Postdoctoral Fellowship. Douglas Kinnison is partially supported by NASA grant no. 80NSSC19K0952. NCAR's Community Earth System Model project is supported primarily by the National Science Foundation. This material is based upon work supported by the National Center for Atmospheric Research, which is a major facility sponsored by the NSF under Cooperative Agreement No. 1852977. Computing and data storage resources, including the Cheyenne supercomputer (doi:10.5065/D6RX99HX), were provided by the Computational and Information Systems Laboratory (CISL) at NCAR. The authors thank the Swedish National Space Agency and the Canadian Space Agency for the continued operation and support of Odin-OSIRIS. Kimberlee

Dube is supported by the Canadian Space Agency (grant no. 21SUASULSO). This project received funding from NOAA's Earth Radiation Budget (ERB) Initiative (CPO #03-01-07-001). Yunqian Zhu is supported in part by NOAA cooperative agreements NA17OAR4320101 and NA22OAR4320151.

Open Research

CESM2/WACCM6 is an open-source community model, which was developed with support primarily from the National Science Foundation. WACCM6 source code can be downloaded at https://www.cesm.ucar.edu/models/cesm2/download. Figures in this study are plotted by using NCAR Command Language (NCL) and Python. The related code can be found in NCL application examples (https://www.ncl.ucar.edu/Applications/). Python is an open-source programming language.

References

Anderson, J. G., Wilmouth, D. M., Smith, J. B., & Sayres, D. S. (2012). UV dosage levels in summer: Increased risk of ozone loss from convectively injected water vapor. *Science*, 337(6096), 835-839. DOI: 10.1126/science.1222978. DOI: 10.1126/science.1222978

Berthet, G., Jégou, F., Catoire, V., Krysztofiak, G., Renard, J. B., Bourassa, A. E., ... & Guimbaud, C. (2017). Impact of a moderate volcanic eruption on chemistry in the lower stratosphere: balloon-borne observations and model calculations. *Atmospheric Chemistry and Physics*, 17(3), 2229-2253. https://doi.org/10.5194/acp-17-2229-2017

Brasseur, G. P., & Solomon, S. (2005). Aeronomy of the middle atmosphere: Chemistry and physics of the stratosphere and mesosphere (Vol. 32). *Springer Science & Business Media*.

Carn, S. A., Krotkov, N. A., Fisher, B. L., & Li, C. (2022). Out of the blue: Volcanic SO2 emissions during the 2021–2022 eruptions of Hunga Tonga—Hunga Ha'apai (Tonga). *Frontiers in Earth Science*, 10, 976962. https://doi.org/10.3389/feart.2022.976962

Carr, J. L., Horváth, Á., Wu, D. L., & Friberg, M. D. (2022). Stereo plume height and motion retrievals for the record-setting Hunga Tonga-Hunga Ha'apai eruption of 15 January 2022. *Geophysical Research Letters*, 49(9), e2022GL098131. https://doi.org/10.1029/2022GL098131

Crutzen, P. J., & Ehhalt, D. H. (1977). Effects of nitrogen fertilizers and combustion on the stratospheric ozone layer. *Ambio*, 112-117.

Douglass, A. R., Schoeberl, M. R., Stolarski, R. S., Waters, J. W., Russell III, J. M., Roche, A. E., & Massie, S. T. (1995). Interhemispheric differences in springtime production of HCl and ClONO2 in the polar vortices. *Journal of Geophysical Research: Atmospheres*, 100(D7), 13967-13978. https://doi.org/10.1029/95JD00698

Dubé, K., Randel, W., Bourassa, A., Zawada, D., McLinden, C., & Degenstein, D. (2020). Trends and variability in stratospheric NOx derived from merged SAGE II and OSIRIS satellite observations. *Journal of Geophysical Research: Atmospheres*, 125(7), e2019JD031798. https:// doi.org/10.1029/2019JD031798

Dubé, K., Zawada, D., Bourassa, A., Degenstein, D., Randel, W., Flittner, D., Sheese, P., and Walker, K.: An improved OSIRIS NO2 profile retrieval in the upper troposphere–lower stratosphere and intercomparison with ACE-FTS and SAGE III/ISS, *Atmos. Meas. Tech*., 15, 6163–6180, https://doi.org/10.5194/amt-15-6163-2022, 2022.

Fahey, D. W., Kawa, S. R., Woodbridge, E. L., Tin, P., Wilson, J. C., Jonsson, H. H., ... & Chan, K. R. (1993). In situ measurements constraining the role of sulphate aerosols in mid-latitude ozone depletion. *Nature*, 363(6429), 509-514. https://doi.org/10.1038/363509a0

Gelaro, R., McCarty, W., Suárez, M. J., Todling, R., Molod, A., Takacs, L., ... & Zhao, B. (2017). The modern-era retrospective analysis for research and applications, version 2 (MERRA-2). *Journal of climate*, 30(14), 5419-5454. https://doi.org/10.1175/JCLI-D-16-0758.1

Gettelman, A., Mills, M. J., Kinnison, D. E., Garcia, R. R., Smith, A. K., Marsh, D. R., ... & Randel, W. J. (2019). The whole atmosphere community climate model version 6 (WACCM6). *Journal of Geophysical Research: Atmospheres*, 124(23), 12380-12403. https://doi.org/10.1029/2019JD030943

Hofmann, D. J., & Solomon, S. (1989). Ozone destruction through heterogeneous chemistry following the eruption of El Chichon. *Journal of Geophysical Research: Atmospheres*, 94(D4), 5029-5041. https://doi.org/10.1029/JD094iD04p05029

Khaykin, S., Podglajen, A., Ploeger, F., Grooß, J. U., Tencé, F., Bekki, S., ... & Ravetta, F. (2022). Global perturbation of stratospheric water and aerosol burden by Hunga eruption. *Communications Earth & Environment*, 3(1), 316. https://doi.org/10.1038/s43247-022-00652-x

Kinnison, D. E., Grant, K. E., Connell, P. S., Rotman, D. A., & Wuebbles, D. J. (1994). The chemical and radiative effects of the Mount Pinatubo eruption. *Journal of Geophysical Research: Atmospheres*, 99(D12), 25705-25731. https://doi.org/10.1029/94JD02318

Krueger, A. J., Walter, L. S., Bhartia, P. K., Schnetzler, C. C., Krotkov, N. A., Sprod, I. T., & Bluth, G. J. S. (1995). Volcanic sulfur dioxide measurements from the total ozone mapping spectrometer instruments. *Journal of Geophysical Research*: Atmospheres, 100(D7), 14057-14076. https://doi.org/10.1029/98GL00178

Ivy, D. J., Solomon, S., Kinnison, D., Mills, M. J., Schmidt, A., & Neely III, R. R. (2017). The influence of the Calbuco eruption on the 2015 Antarctic ozone hole in a fully coupled chemistry-climate model. *Geophysical Research Letters*, 44(5), 2556-2561. https://doi.org/10.1002/2016GL071925

Legras, B., Duchamp, C., Sellitto, P., Podglajen, A., Carboni, E., Siddans, R., ... & Ploeger, F. (2022). The evolution and dynamics of the Hunga Tonga–Hunga Ha'apai sulfate aerosol plume in the stratosphere. *Atmospheric Chemistry and Physics*, 22(22), 14957-14970. https://doi.org/10.5194/acp-22-14957-2022

Lin, S. J., & Rood, R. B. (1996). Multidimensional flux-form semi-Lagrangian transport schemes. *Monthly Weather Review*, 124(9), 2046-2070. https://doi.org/10.1175/1520-0493(1996)124<2046:MFFSLT>2.0.CO;2

Livesey, N J, W G Read, P A Wagner, L Froidevaux, M L Santee, and M J Schwartz. 2020. "Version 5.0 x Level 2 and 3 Data Quality and Description Document (Tech. Rep. No. JPL D-105336 Rev. A)." *Jet Propulsion Laboratory*.

Llewellyn, E. J., Lloyd, N. D., Degenstein, D. A., Gattinger, R. L., Petelina, S. V., Bourassa, A. E., Wiensz, J. T., Ivanov, E. V., McDade, I. C., Solheim, B. H., McConnell, J. C., Haley, C. S., von Savigny, C., Sioris, C. E., McLinden, C. A., Griffioen, E., Kaminski, J., Evans, W. F., Puckrin, E., Strong, K., Wehrle, V., Hum, R. H., Kendall, D. J., Matsushita, J., Murtagh, D. P., Brohede, S., Stegman, J., Witt, G., Barnes, G., Payne, W. F., Piché, L., Smith, K., Warshaw, G., Deslauniers, D. L., Marchand, P., Richardson, E. H., King, R. A., Wevers, I., McCreath, W., Kyrölä, E., Oikarinen, L., Leppelmeier, G. W., Auvinen, H., Mégie, G., Hauchecorne, A., Lefèvre, F., de La Nöe, J., Ricaud, P., Frisk, U., Sjoberg, F., von Schéele, F., and Nordh, L.: The OSIRIS instrument on the Odin spacecraft, *Can. J. Phys.*, 82, 411–422, https://doi.org/10.1139/p04-005, 2004.

Lu, J., Lou, S., Huang, X., Xue, L., Ding, K., Liu, T., ... & Ding, A. (2023). Stratospheric Aerosol and Ozone Responses to the Hunga Tonga-Hunga Ha'apai Volcanic Eruption. *Geophysical Research Letters*, 50(4), e2022GL102315. https://doi.org/10.1029/2022GL102315

Manney, G. L., Santee, M. L., Lambert, A., Millan, L., Minschwaner, K., Werner, F., ... & Wang, T. (2023). Siege of the South: Hunga Tonga-Hunga Ha'apai Water Vapor Excluded from 2022 Antarctic Stratospheric Polar Vortex. *Authorea Preprints*. 10.22541/essoar.168057560.00140372/v1

McLinden, C. A., Olsen, S. C., Hannegan, B., Wild, O., Prather, M. J., & Sundet, J. (2000). Stratospheric ozone in 3-D models: A simple chemistry and the cross-tropopause flux. *Journal of Geophysical Research*, 105(D11), 14653–14665. https://doi.org/10.1029/2000JD900124

Mills, M. J., Langford, A. O., O'Leary, T. J., Arpag, K., Miller, H. L., Proffitt, M. H., ... & Solomon, S. (1993). On the relationship between stratospheric aerosols and nitrogen dioxide. *Geophysical research letters*, 20(12), 1187-1190. https://doi.org/10.1029/93GL01124

Mills, M. J., Schmidt, A., Easter, R., Solomon, S., Kinnison, D. E., Ghan, S. J., ... & Gettelman, A. (2016). Global volcanic aerosol properties derived from emissions, 1990–2014, using

CESM1 (WACCM). *Journal of Geophysical Research: Atmospheres*, 121(5), 2332-2348. https://doi.org/10.1002/2015JD024290

Mills, M. J., Richter, J. H., Tilmes, S., Kravitz, B., MacMartin, D. G., Glanville, A. A., ... & Kinnison, D. E. (2017). Radiative and chemical response to interactive stratospheric sulfate aerosols in fully coupled CESM1 (WACCM). *Journal of Geophysical Research: Atmospheres*, 122(23), 13-061. https://doi.org/10.1002/2017JD027006

Millan, L., Santee, M. L., Lambert, A., Livesey, N. J., Werner, F., Schwartz, M. J., ... & Froidevaux, L. (2022). The Hunga Tonga-Hunga Ha'apai hydration of the stratosphere. *Geophysical Research Letters*, 49(13), e2022GL099381. https://doi.org/10.1029/2022GL099381

Murtagh, D., Frisk, U., Merino, F., Ridal, M., Jonsson, A., Stegman, J., Witt, G., Eriksson, P., Jiménez, C., Megie, G., Noë, J. d. l., Ricaud, P., Baron, P., Pardo, J. R., Hauchcorne, A., Llewellyn, E. J., Degenstein, D. A., Gattinger, R. L., Lloyd, N. D., Evans, W. F., McDade, I. C., Haley, C. S., Sioris, C., Savigny, C. v., Solheim, B. H., McConnell, J. C., Strong, K., Richardson, E. H., Leppelmeier, G. W., Kyrölä, E., Auvinen, H., and Oikarinen, L.: An overview of the Odin atmospheric mission, *Can. J. Phys.*, 80, 309–319, https://doi.org/10.1139/p01-157, 2002.

Park, M., Randel, W. J., Kinnison, D. E., Bourassa, A. E., Degenstein, D. A., Roth, C. Z., ... & Santee, M. L. (2017). Variability of stratospheric reactive nitrogen and ozone related to the QBO. *Journal of Geophysical Research: Atmospheres*, 122(18), 10-103. https://doi.org/10.1002/2017JD027061

Portmann, R. W., Solomon, S., Garcia, R. R., Thomason, L. W., Poole, L. R., & McCormick, M. P. (1996). Role of aerosol variations in anthropogenic ozone depletion in the polar regions. *Journal of Geophysical Research: Atmospheres*, 101(D17), 22991-23006. https://doi.org/10.1029/96JD02608

Prather, M., & Jaffe, A. H. (1990). Global impact of the Antarctic ozone hole: Chemical propagation. *Journal of Geophysical Research,* 95(D4), 3473–3492. https://doi.org/10.1029/JD095iD04p03473

Proud, S. R., Prata, A. T., & Schmauß, S. (2022). The January 2022 eruption of Hunga Tonga-Hunga Ha'apai volcano reached the mesosphere. *Science*, 378(6619), 554-557. DOI: 10.1126/science.abo4076

Randel, W. J., Johnston, B. R., Braun, J. J., Sokolovskiy, S., Vömel, H., Podglajen, A., & Legras, B. (2023). Stratospheric Water Vapor from the Hunga Tonga–Hunga Ha'apai Volcanic Eruption Deduced from COSMIC-2 Radio Occultation. *Remote Sensing*, 15(8), 2167. https://doi.org/10.3390/rs15082167

Read, W. G., Froidevaux, L., & Waters, J. W. (1993). Microwave limb sounder measurement of stratospheric SO2 from the Mt. Pinatubo Volcano. *Geophysical Research Letters*, 20(12), 1299-1302. https://doi.org/10.1029/93GL00831

Santee, M. L., Lambert, A., Froidevaux, L., Manney, G. L., Schwartz, M. J., Millan, L., ... & Fuller, R. A. (2023). Strong Evidence of Heterogeneous Processing on Stratospheric Sulfate Aerosol in the Extrapolar Southern Hemisphere Following the 2022 Hunga Tonga-Hunga Ha'apai Eruption. *Authorea Preprints*. DOI: 10.22541/essoar.168500358.84889871/v1

Schoeberl, M. R., Wang, Y., Ueyama, R., Taha, G., Jensen, E., & Yu, W. (2022). Analysis and impact of the Hunga Tonga-Hunga Ha'apai stratospheric water vapor plume. *Geophysical Research Letters*, 49(20), e2022GL100248. https://doi.org/10.1029/2022GL100248

Stimpfle, R. M., Koplow, J. P., Cohen, R. C., Kohn, D. W., Wennberg, P. O., Judah, D. M., ... & Chan, K. R. (1994). The response of ClO radical concentrations to variations in NO2 radical concentrations in the lower stratosphere. *Geophysical research letters*, 21(23), 2543-2546. https://doi.org/10.1029/94GL02373

Stone, K. A., Solomon, S., Kinnison, D. E., Pitts, M. C., Poole, L. R., Mills, M. J., ... & Hagiya, S. (2017). Observing the impact of Calbuco volcanic aerosols on South Polar ozone depletion in 2015. *Journal of Geophysical Research: Atmospheres*, 122(21), 11-862. https://doi.org/10.1002/2017JD026987

Solomon, S., Portmann, R. W., Garcia, R. R., Thomason, L. W., Poole, L. R., & McCormick, M. P. (1996). The role of aerosol variations in anthropogenic ozone depletion at northern midlatitudes. *Journal of Geophysical Research: Atmospheres*, 101(D3), 6713-6727. https://doi.org/10.1029/95JD03353

Solomon, S., Borrmann, S., Garcia, R. R., Portmann, R., Thomason, L., Poole, L. R., ... & McCormick, M. P. (1997). Heterogeneous chlorine chemistry in the tropopause region. *Journal of Geophysical Research: Atmospheres*, 102(D17), 21411-21429. https://doi.org/10.1029/97JD01525

Solomon, S., Portmann, R. W., Garcia, R. R., Randel, W., Wu, F., Nagatani, R., ... & McCormick, M. P. (1998). Ozone depletion at mid-latitudes: Coupling of volcanic aerosols and temperature variability to anthropogenic chlorine. *Geophysical Research Letters*, 25(11), 1871-1874. https://doi.org/10.1029/98GL01293

Solomon, S. (1999). Stratospheric ozone depletion: A review of concepts and history. *Reviews of geophysics*, 37(3), 275-316. https://doi.org/10.1029/1999RG900008

Solomon, S., Portmann, R. W., Sasaki, T., Hofmann, D. J., & Thompson, D. W. (2005). Four decades of ozonesonde measurements over Antarctica. *Journal of Geophysical Research: Atmospheres*, 110(D21). https://doi.org/10.1029/2005JD005917

Solomon, S., Kinnison, D., Bandoro, J., & Garcia, R. (2015). Simulation of polar ozone depletion: An update. *Journal of Geophysical Research: Atmospheres*, 120(15), 7958-7974. https://doi.org/10.1002/2015JD023365

Solomon, S., Ivy, D. J., Kinnison, D., Mills, M. J., Neely III, R. R., & Schmidt, A. (2016). Emergence of healing in the Antarctic ozone layer. *Science*, 353(6296), 269-274. DOI: 10.1126/science.aae0061

Stone, K. A., Solomon, S., Kinnison, D. E., Pitts, M. C., Poole, L. R., Mills, M. J., ... & Hagiya, S. (2017). Observing the impact of Calbuco volcanic aerosols on South Polar ozone depletion in 2015. *Journal of Geophysical Research: Atmospheres*, 122(21), 11-862. https://doi.org/10.1002/2017JD026987

Taha, G., Loughman, R., Colarco, P. R., Zhu, T., Thomason, L. W., & Jaross, G. (2022). Tracking the 2022 Hunga Tonga-Hunga Ha'apai aerosol cloud in the upper and middle stratosphere using space-based observations. *Geophysical Research Letters*, 49(19), e2022GL100091. https://doi.org/10.1029/2022GL100091

Tie, X., & Brasseur, G. (1995). The response of stratospheric ozone to volcanic eruptions: Sensitivity to atmospheric chlorine loading. *Geophysical Research Letters*, 22(22), 3035-3038. https://doi.org/10.1029/95GL03057

Vömel, H., Evan, S., & Tully, M. (2022). Water vapor injection into the stratosphere by Hunga Tonga-Hunga Ha'apai. *Science*, 377(6613), 1444-1447. DOI: 10.1126/science.abq2299

Wang, X., Randel, W., Zhu, Y., Tilmes, S., Starr, J., Yu, W., ... & Li, J. (2022). Stratospheric climate anomalies and ozone loss caused by the Hunga Tonga volcanic eruption. *Authorea Preprints*. DOI: 10.1002/essoar.10512922.1

Wennberg, P. O., Cohen, R. C., Stimpfle, R. M., Koplow, J. P., Anderson, J. G., Salawitch, R. J., ... & Wofsy, S. C. (1994). Removal of stratospheric O3 by radicals: In situ measurements of OH, HO2, NO, NO2, ClO, and BrO. *Science*, 266(5184), 398-404. DOI: 10.1126/science.266.5184.398

Xu, J., Li, D., Bai, Z., Tao, M., & Bian, J. (2022). Large amounts of water vapor were injected into the stratosphere by the hunga tonga–hunga ha'apai volcano eruption. *Atmosphere*, 13(6), 912. https://doi.org/10.3390/atmos13060912

Zambri, B., LeGrande, A. N., Robock, A., & Slawinska, J. (2017). Northern Hemisphere winter warming and summer monsoon reduction after volcanic eruptions over the last millennium. *Journal of Geophysical Research: Atmospheres*, 122(15), 7971-7989. https://doi.org/10.1002/2017JD026728

Zambri, B., Solomon, S., Kinnison, D. E., Mills, M. J., Schmidt, A., Neely III, R. R., ... & Roth, C. Z. (2019). Modeled and observed volcanic aerosol control on stratospheric NOy and

Cly. *Journal of Geophysical Research: Atmospheres*, 124(17-18), 10283-10303. https://doi.org/10.1029/2019JD031111

Zhang, J., Wuebbles, D., Kinnison, D., & Baughcum, S. L. (2021). Stratospheric ozone and climate forcing sensitivity to cruise altitudes for fleets of potential supersonic transport aircraft. *Journal of Geophysical Research: Atmospheres,* 126(16), e2021JD034971. https://doi.org/10.1029/2021JD034971

Zhu, Y., Toon, O. B., Kinnison, D., Harvey, V. L., Mills, M. J., Bardeen, C. G., ... & Jégou, F. (2018). Stratospheric aerosols, polar stratospheric clouds, and polar ozone depletion after the Mount Calbuco eruption in 2015. *Journal of Geophysical Research: Atmospheres*, 123(21), 12-308. https://doi.org/10.1029/2018JD028974

Zhu, Y., Bardeen, C. G., Tilmes, S., Mills, M. J., Wang, X., Harvey, V. L., ... & Toon, O. B. (2022). Perturbations in stratospheric aerosol evolution due to the water-rich plume of the 2022 Hunga-Tonga eruption. *Communications Earth & Environment*, 3(1), 248. https://doi.org/10.1038/s43247-022-00580-w

Geophysical Research Letters

Supporting Information for

Chemistry contribution on stratospheric ozone depletion after the unprecedented water rich Hunga Tonga eruption

Authors: Jun Zhang[1*], Douglas Kinnison[1], Yunqian Zhu[2,3], Xinyue Wang[1], Simone Tilmes[1], Kimberlee Dube[4], William Randel[1]

Affiliations:

[1]Atmospheric Chemistry Observations & Modeling Laboratory, National Center for Atmospheric Research, Boulder, CO, USA

[2] Cooperative Institute for Research in Environmental Sciences, University of Colorado Boulder, Boulder, CO, USA, 80309

[3]Chemical Sciences Laboratory, National Oceanic and Atmospheric Administration, Boulder, CO, USA, 80305

[4]Institute of Space and Atmospheric Studies, University of Saskatchewan, Saskatoon, SK, Canada

[*]Corresponding author: Jun Zhang (jzhan166@ucar.edu)

Contents of this file

Introduction

Supporting information includes text and figures to support the discussion in the main article.

Text S1. Odd oxygen definition and reactions included in each odd-oxygen loss mechanism.

Odd oxygen definition Ox = O_3 + $O(^3P)$ + O(1D) + NO_2 + $2NO_3$ + HNO_3 + HO_2NO_2 + $2N_2O_5$ + ClO + $2Cl_2O_2$ + 2OClO + $2ClONO_2$ + BrO + $2BrONO_2$, which is approximately equal to O_3 + $O(^3P)$

Chapman mechanism self-loss cycle, plus O1D_H2O (Ox-Ox):
OddOx_Ox_Loss = 2.*($O+O_3$) + ($O(^1D)+H_2O$)

NOx involved Ox loss cycle (NOx-Ox):
OddOx_NOx_Loss = 2*(NO_2+O) + 2*(NO_3+hv)

HOx involved Ox loss cycle (HOx-Ox):
OddOx_HOx_Loss = (HO_2+O) + (HO_2+O_3) + (OH+O) + ($OH+O_3$) + ($H+O_3$)

ClOx/BrOx involved Ox loss cycle (ClOx/BrOx-Ox):
OddOx_CLOxBROx_Loss = 2*(ClO+O) + 2*(2*(ClOOCl + hv) + 2*(ClO+ClO=> 2Cl + O_2) + 2*(ClO+ClO => Cl_2 + O_2) + 2*(BrO+ClO => Br + Cl + O_2) + 2*(BrO+ClO => BrCl + O_2) + 2*(BrO+BrO) + 2*(BrO+O) + (ClO+HO_2) + (BrO+HO_2)

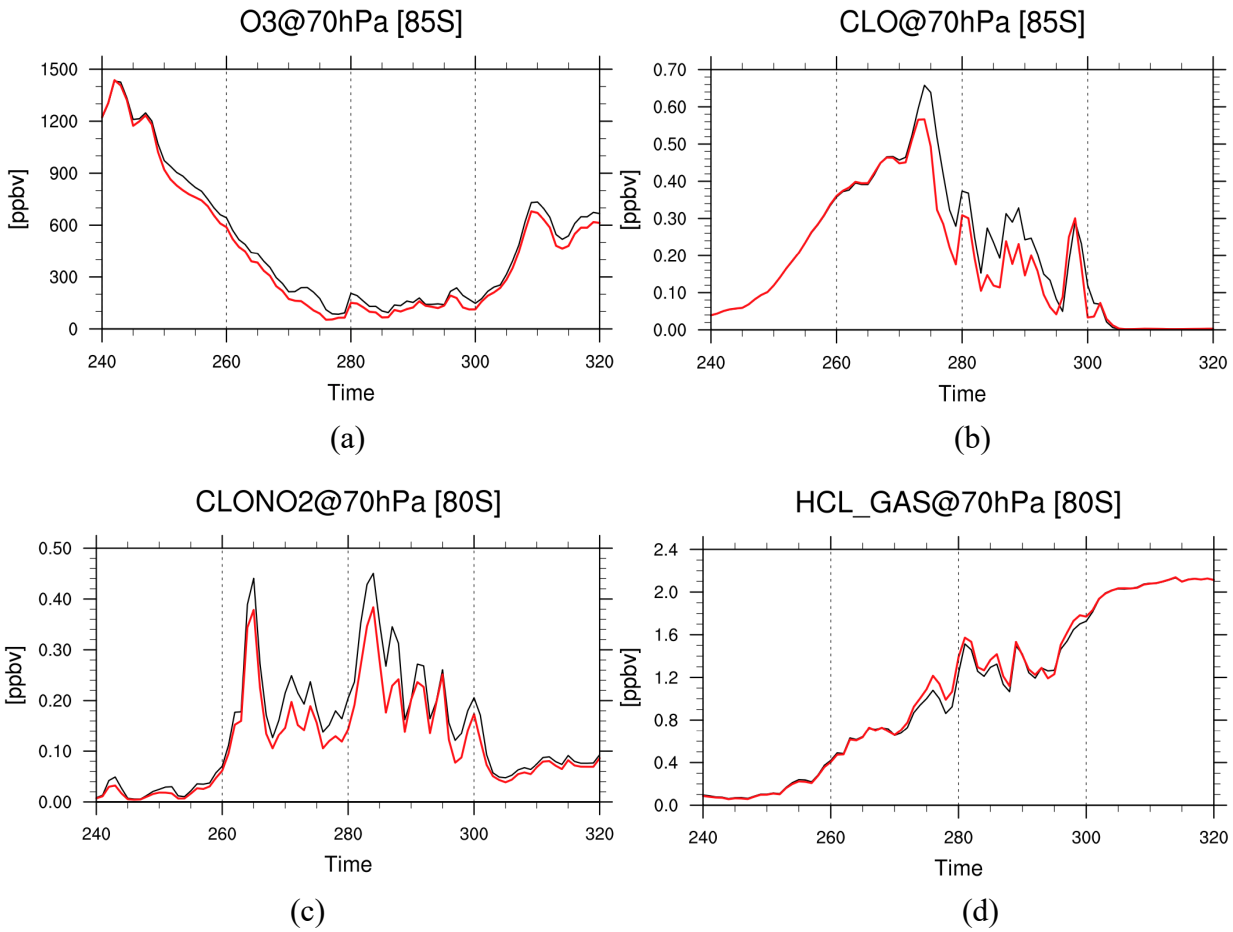

Figure S1. Calculated perturbations from full-forcing (SO_2+H_2O) experiment run (red lines) compared to no-forcing control runs (black lines) for (a) O_3 (b) ClO (c) $ClONO_2$ and (d) HCl at 70 hPa 80°S. Shown day 240 to 320 in 2022.

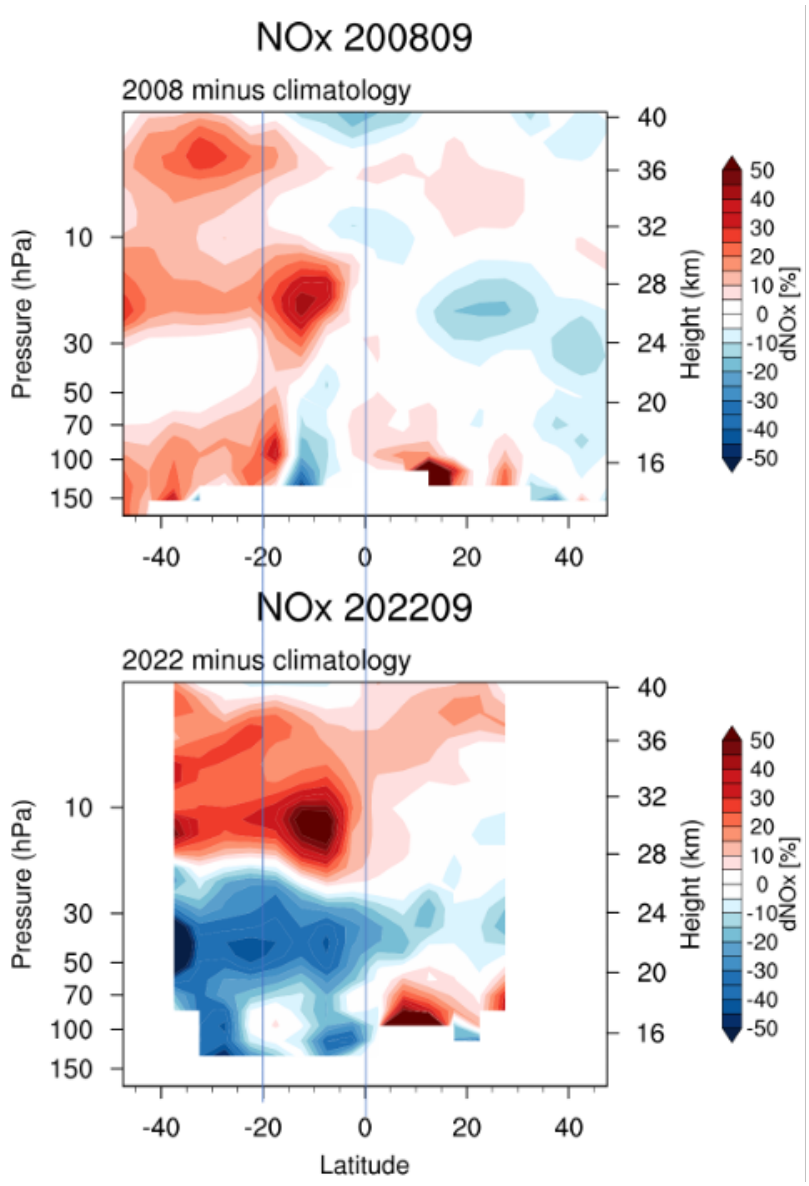

70
71

72 **Figure S2.** Calculated NOx anomaly (%) relative to climatology (2007 to 2021) from OSIRIS in
73 September 2008 (top) and 2022 (bottom).

74